

AD-A043 690

BOLT BERANEK AND NEWMAN INC CAMBRIDGE MASS

F/G 17/A

A MODEL FOR THE PILOT'S USE OF MOTION CUES IN ROLL-AXIS TRACKIN--ETC(U)

JUN 77 W H LEVISON, A M JUNKER

F44620-75-C-0060

UNCLASSIFIED

BBN-3528

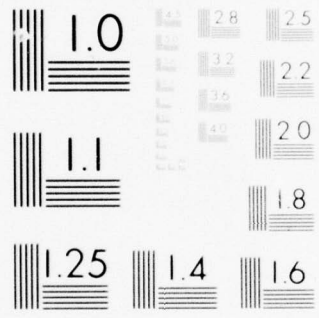
AMRL-TR-77-40

NL

| OF |  
AD  
A043690



END  
DATE  
FILMED  
9-77  
DDC



MICROCOPY RESOLUTION TEST CHART  
NATIONAL BUREAU OF STANDARDS-1963-A

ADA 043690

AMRL-TR-77-40

12  
NW



# A MODEL FOR THE PILOT'S USE OF MOTION CUES IN ROLL-AXIS TRACKING TASKS

WILLIAM H. LEVISON  
BOLT BERANEK & NEWMAN, INC.  
CAMBRIDGE, MASSACHUSETTS 02138

ANDREW M. JUNKER  
AEROSPACE MEDICAL RESEARCH LABORATORY

JUNE 1977

DDC  
RECEIVED  
SEP 1 1977  
RECEIVED  
R

Approved for public release; distribution unlimited.

AD No. \_\_\_\_\_  
DDC FILE COPY

AEROSPACE MEDICAL RESEARCH LABORATORY  
AEROSPACE MEDICAL DIVISION  
AIR FORCE SYSTEMS COMMAND  
WRIGHT-PATTERSON AIR FORCE BASE, OHIO 45433

## NOTICES

When US Government drawings, specifications, or other data are used for any purpose other than a definitely related Government procurement operation, the Government thereby incurs no responsibility nor any obligation whatsoever, and the fact that the Government may have formulated, furnished, or in any way supplied the said drawings, specifications, or other data, is not to be regarded by implication or otherwise, as in any manner licensing the holder or any other person or corporation, or conveying any rights or permission to manufacture, use, or sell any patented invention that may in any way be related thereto.

Please do not request copies of this report from Aerospace Medical Research Laboratory. Additional copies may be purchased from:

National Technical Information Service  
5285 Port Royal Road  
Springfield, Virginia 22161

Federal Government agencies and their contractors registered with Defense Documentation Center should direct requests for copies of this report to:

Defense Documentation Center  
Cameron Station  
Alexandria, Virginia 22314

## TECHNICAL REVIEW AND APPROVAL

AMRL-TR-77-40

This report has been reviewed by the Information Office (OI) and is releasable to the National Technical Information Service (NTIS). At NTIS, it will be available to the general public, including foreign nations.

This technical report has been reviewed and is approved for publication.

**FOR THE COMMANDER**



CLYDE R. REPLOGLE, PhD  
Chief  
Environmental Medicine Division  
Aerospace Medical Research Laboratory

SECURITY CLASSIFICATION OF THIS PAGE (When Data Entered)

REPORT DOCUMENTATION PAGE		READ INSTRUCTIONS BEFORE COMPLETING FORM
1. REPORT NUMBER <b>18</b> AMRL-TR-77-40 ✓	2. GOVT ACCESSION NO.	3. RECIPIENT'S CATALOG NUMBER <b>9</b>
4. TITLE (and Subtitle) <b>5</b> A MODEL FOR THE PILOT'S USE OF MOTION CUES IN ROLL-AXIS TRACKING TASKS		5. TYPE OF REPORT & PERIOD COVERED Interim Scientific Report
7. AUTHOR(s) <b>10</b> William H. Levison* Andrew M. Junker**		6. PERFORMING ORG. REPORT NUMBER <b>14</b> BBN Report No - 3528
9. PERFORMING ORGANIZATION NAME AND ADDRESS *Bolt Beranek and Newman Inc. Cambridge, Massachusetts 02138		8. CONTRACT OR GRANT NUMBER(s) <b>15</b> F44620-75-C-0060 ✓
11. CONTROLLING OFFICE NAME AND ADDRESS Air Force Office of Scientific Research Bolling Air Force Base, DC 20332		10. PROGRAM ELEMENT, PROJECT, TASK AREA & WORK UNIT NUMBERS <b>16</b> 61102F, 2312-V2-17
14. MONITORING AGENCY NAME & ADDRESS (if different from Controlling Office) **Aerospace Medical Research Laboratory, Aerospace Medical Division, Air Force Systems Command, Wright-Patterson Air Force Base, Ohio 45433		12. REPORT DATE <b>11</b> June 1977 <b>12</b> V2
		13. NUMBER OF PAGES 80
		15. SECURITY CLASS. (of this report) Unclassified
		15a. DECLASSIFICATION/DOWNGRADING SCHEDULE n/a
16. DISTRIBUTION STATEMENT (of this Report) <b>128 pp.</b> Approved for public release; distribution unlimited		
17. DISTRIBUTION STATEMENT (of the abstract entered in Block 20, if different from Report)		
18. SUPPLEMENTARY NOTES		
19. KEY WORDS (Continue on reverse side if necessary and identify by block number) human operator technology human operator modeling motion optimal control model		
20. ABSTRACT (Continue on reverse side if necessary and identify by block number) An experimental and analytical study was undertaken jointly by the Aerospace Medical Research Laboratory and Bolt Beranek and Newman Inc. to test a model for the pilot's use of motion cues in roll-axis tracking tasks. Simulated target-following and disturbance-regulations tasks were explored with subjects using visual-only and combined visual and motion cues. The effects of motion cues on task performance and pilot response behavior were appreciably different for the two task configurations and were consistent with data reported in earlier studies for similar task configurations.		

DDC  
RECEIVED  
SEP 1 1977  
RECEIVED  
B

060100

1B

Block 20. Cont'd

→ The "optimal-control" model for pilot/vehicle systems provided a task-independent framework for accounting for the pilot's use of motion cues. Specifically, the availability of motion cues was modeled by augmenting the set of perceptual variables to include position, rate, acceleration, and acceleration-rate of the motion simulator; and results were consistent with the hypothesis of attention-sharing between visual and motion variables. This straightforward informational model allowed accurate model predictions of the effects of motion cues on a variety of response measures for both the target-following and disturbance-regulation tasks.

PREFACE

The work reported herein was performed in part under AFOSR Contract No. F44620-75-C-0060. Technical Monitors for the Air Force were Lt. Col. William Wisecup and Lt. Col. Dominic Maio of the Air Force Office of Scientific Research.

This Interim Scientific Report summarizes the work performed by Bolt Beranek and Newman Inc. during the second year of a joint study conducted in conjunction with the Aerospace Medical Research Laboratory (AMRL) under AFOSR Contract No. F44620-75-C-0060. The results of the first-year effort have been documented by Levison, Baron, and Junker [1].

ACCESSION for		
NTIS	White Section	<input checked="" type="checkbox"/>
DDC	Buff Section	<input type="checkbox"/>
UNANNOUNCED		<input type="checkbox"/>
JUSTIFICATION _____		
BY _____		
DISTRIBUTION/AVAILABILITY CODES		
Dist.	AVAIL.	and/or SPLCIAL
A		

TABLE OF CONTENTS

<u>Section</u>	<u>Page</u>
1. INTRODUCTION. . . . .	5
2. BACKGROUND. . . . .	6
2.1 Review of the Preceding Study. . . . .	7
2.2 Further Analysis . . . . .	9
3. DESCRIPTION OF EXPERIMENTS. . . . .	18
3.1 Description of the Tasks . . . . .	18
3.2 Experimental Procedure . . . . .	26
4. EXPERIMENTAL RESULTS. . . . .	25
4.1 Primary Data Reduction . . . . .	25
4.2 Model Analysis . . . . .	36
5. CONCLUSIONS . . . . .	54
APPENDIX A - ANALYSIS PROCEDURES. . . . .	56
APPENDIX B - ADDITIONAL EXPERIMENTAL RESULTS. . . . .	61
APPENDIX C - MODEL FORMULATION. . . . .	69
REFERENCES. . . . .	75

## LIST OF FIGURES

<u>Figure</u>		<u>Page</u>
1.	Effect of Sensor Dynamics on Predicted Rms Performance Scores. . . . .	12
2.	Effect of Sensor Dynamics on Predicted Frequency Response. . . . .	13
3.	Block Diagram of the Tracking Task. . . . .	21
4.	Sketch of the Central Display . . . . .	21
5.	Effect of Motion Cues on Rms Performance Scores . . .	29
6.	Effect of Motion Cues on Pilot Frequency Response . .	31
7.	Comparison of Typical and Mean Responses. . . . .	34
8.	Comparison of Model and Experimental Performance Scores. . . . .	41
9.	Comparison of Model and Experimental Frequency Response. . . . .	42
10.	Matching Errors for Various Hypotheses. . . . .	45
11.	Effect of Acceleration-Rate Perception on Predicted Performance . . . . .	47
12.	Comparison of Model and Experimental Rms Error Scores for Two Studies. . . . .	53
A-1.	Flow Diagram of the Tracking Task . . . . .	57

LIST OF TABLES

<u>Table</u>		<u>Page</u>
1.	Multi-Axis Tracking Simulator: Roll-Axis Characteristics. . . . .	19
2.	Tracking Variables Analyzed. . . . .	28
3.	Coding for Significance Level. . . . .	28
4.	Effects of Motion Cues on Frequency Response . . . .	32
5.	Values for Pilot-Related Model Parameters. . . . .	38
B-1	Effect of Motion Cues on Performance Costs . . . . .	62
B-2	Effect of Motion Cues on Rms Performance Scores. . .	63
B-3	Effect of Motion Cues on Pilot Describing Function, Target Input . . . . .	64
B-4	Effect of Motion Cues on Pilot Describing Function, Disturbance Input. . . . .	65
B-5	Effect of Motion Cues on Remnant Ratio . . . . .	66

## 1. INTRODUCTION

Two tasks were performed in the preceding study phase: (1) the "optimal control" pilot/vehicle model was modified to provide an alternative treatment of motor-related sources of pilot randomness, and (2) the revised model was used to analyze the pilot's use of motion cues in a series of roll-axis tracking experiments. A simple informational treatment of motion cues provided a consistent explanation of the performance differences between the motion and no-motion conditions explored in the study.

The effects of motion cues found in the first-year study differed qualitatively from those reported by earlier investigators. Therefore, a second set of experiments was performed to resolve these apparent discrepancies; the results of these experiments are the major topic of this report.

The results of the first-year study effort under this contract are reviewed in the following section, and some additional model results are presented. Section 3 contains a description of the experiments conducted in the second-year effort; the results of primary data reduction and model analysis are presented in Section 4. Section 5 summarizes the results of this effort.

Appendix A provides supplementary information relating to data analysis. Detailed experimental results not presented in the main text are tabulated in Appendix B, and Appendix C contains certain details related to problem formulation for model analysis.

The reader is assumed to be familiar with the information contained in the preceding Interim Report [1]. Readers not familiar with the optimal-control pilot/vehicle model employed in this study are referred to the preceding report for an illustration of model application and to the references contained in that report for additional details on model theory and application.

## 2. BACKGROUND

Results of the preceding study phase are described below, and some additional analysis of the data obtained in that study is presented.

### 2.1 Review of the Preceding Study

#### 2.1.1 Model Revisions

Modifications to the pilot model consisted of a revised treatment of motor-related sources of pilot randomness (or "remnant"). Specifically, (1) motor noise was treated as a wide-band process added to control rate, rather than to commanded control as had been done previously, and (2) the concept of "pseudo" motor noise was introduced to allow a differentiation between the actual noise driving the system ("driving" motor noise) and the pilot's internal model of this noise (the "pseudo" noise). No modifications were made to the model structure specifically to treat the pilot's use of motion cues.

Adding motor noise to control rate allowed the model to reproduce the low-frequency "phase-droop" exhibited by most pilot describing functions. Although tracking performance is generally little affected by low-frequency phase response, it was necessary to obtain an accurate model of this aspect of controller behavior because of the importance of low-frequency phase characteristics on performance in the AMRL/BBN roll-axis tracking study. By introducing the concept of pseudo motor noise, we gained added flexibility in representing pilot uncertainties about his own control behavior and about vehicle response. The mathematical implications of this model revision,

as well as applications of the revised model to previous laboratory tracking results, are documented in Levison, Baron, and Junker [1].

### 2.2.1 Analysis of Motion Cues

An experimental and analytical study was performed jointly by AMRL and BBN. Experiments were performed at AMRL. Primary data reduction was performed by the Air Force; statistical analysis and modeling were performed by Bolt Beranek and Newman Inc. (BBN). The results of this study are documented in Levison, Baron, and Junker [1] and Levison [2].

This study was concerned with the use of motion-related sensory information for continuous flight control. Other potential effects of motion, such as providing alerting cues to the pilot or providing "realism" to aircraft simulations, were not considered. Analysis of the experimental results was directed towards developing a generalized description of the manner in which the pilot uses motion cues, with the ultimate goal of providing a model that can predict the effects of motion cues on system performance in a variety of control situations.

The revised pilot model was used as the basis for modeling the use of motion cues. Model analysis was directed towards finding the most straightforward set of rules for adjusting pilot-related parameters that would reliably account for the effects of motion cues on pilot response and total system performance.

The principal results of this study were as follows:

1. The effects of motion cues on roll-axis tracking performance were modeled primarily by (a) inclusion of sensory variables that are likely to be provided by motion sensors (position, rate, and acceleration of the controlled vehicle in these experiments), and (b) an increment of 0.05 seconds to the pilot time delay. Modeling of dynamics associated with motion sensing was not required.
2. The experimental results did not allow us to determine whether motion and visual cues were processed in parallel without interference, or whether the pilot had to "share attention" between modalities. Furthermore, we were unable to determine whether the pilot obtained only rate cues from his motion sensors, or whether he used a combination of position, rate, and acceleration cues.
3. Tracking performance was consistent with the notion that attention was shared optimally. Moreover, model analysis indicated that optimal allocation of attention between visual and motion cues was different for the two control tasks explored in the AMRL study.
4. Although tracking error was not greatly affected by the selection of a relative performance penalty on control-rate activity, a good match to control scores required readjustment of this penalty for the two plants explored in the study; furthermore, different weightings were found for motion and static tracking for the more difficult plant.

5. The results of the AMRL study differed in certain respects from earlier studies of motion-based tracking. In the AMRL study, availability of motion cues resulted in an increase of low-frequency phase lead, an increase in high-frequency phase lag, and no important change in gain-crossover frequency; whereas earlier studies have shown that motion has little effect on low-frequency phase lead, reduces high-frequency phase lag, and allows an increase in gain-crossover frequency.
6. Although motion cues did not enhance tracking performance for the less difficult plant explored in the AMRL study, model analysis predicts that motion will enhance task performance if the pilot is required to allocate a substantial fraction of his attention to another task. That is, the less attention paid to the tracking task, the greater should be the relative benefit of motion cues.

## 2.2 Further Analysis

### 2.2.1 Effects of Motion Sensor Dynamics

One of the questions raised by the preceding study was whether or not an adequate match could be obtained to the AMRL/BBN results using existing models for vestibular motion sensors. If an adequate match could not be obtained, we would have to conclude that either (1) existing models for vestibular sensors were inadequate, or (2) that non-vestibular motion cues were important. If, on the other hand, a superior match could be obtained, we would establish the necessity for including sensor submodels in

the overall pilot/vehicle model. Finally, if inclusion of vestibular models did not significantly affect the matching capability of the model, we would simply conclude that such models were not required for modeling pilot performance in tasks of the sort explored in the experimental study.

The following models were included in the pilot/vehicle representation to account for the dynamical response properties of vestibular motion sensors. Response characteristics for the semicircular canals, obtained from Peters [3], was

$$Y_s = \frac{10}{(s + 0.1)(s + 10)} \dot{\omega} \quad (1)$$

where  $y_s$  is the sensation provided to the pilot by the semicircular canals, and  $\dot{\omega}$  is rotational acceleration. Response characteristics of the otolith, obtained from Young [4], were assumed to be

$$Y_o = \frac{1.5(s + 0.076)}{(s + 0.19)(s + 1.5)} SF \quad (2)$$

where  $y_o$  is the sensation provided by the utricles and SF is the motion input considered as a specific force. Since the subject's head was located approximately on the axis of rotation of the simulator, translational acceleration of the head was assumed to be negligible, and the major input was assumed to be tilt. Therefore, the effective input to the otoliths was assumed to be roll angle.

The results of "Task 2" - the more difficult of the two tasks explored in the AMRL/BBN study - were reanalyzed. The basic pilot model was augmented by inclusion of these dynamics in the description of system response behavior, and the

"display vector" consisted of four quantities: roll angle and roll angle rate, obtained visually, and the quantities  $y_s$  and  $y_o$  provided by the motion sensors.

Pilot parameters of control-rate weighting, pseudo motor noise/signal ratio, and observation noise/signal ratio were selected as shown in Table 1 of Levison, Baron and Junker for the Task 2 motion experiment. Time delay was treated as a variable of the analysis, and "attention" to the various perceptual quantities was manipulated according to the hypotheses of (1) interference between motion and visual perceptions, and (2) no interference. Model-matching scores along various dimensions were computed as defined in [1].

As in the preceding analysis, no single set of pilot parameters provided the best match along all measurement dimensions. That is, one set of parameters provided the best overall match to rms performance scores, another to the pilot describing function, etc. A good match - one comparable to that obtained in the preceding study - was obtained with a time delay of 0.22 seconds and an attentional split of 60% to visual cues and 40% to motion cues. (Analysis with the non-dynamical model for motion cues yielded a time delay of 0.25 seconds and 70%-30% attention split.)

As shown in Figures 1 and 2, the model including the motion sensor dynamics provided predictions nearly identical to those provided by the simple informational model that did not include such dynamics. We therefore conclude that, while models of vestibular dynamics are consistent with the results obtained experimentally, model accuracy is not enhanced by the consideration of such models. For the type of tasks explored in the AMRL/BBN study, a simple informational analysis appears to be adequate.

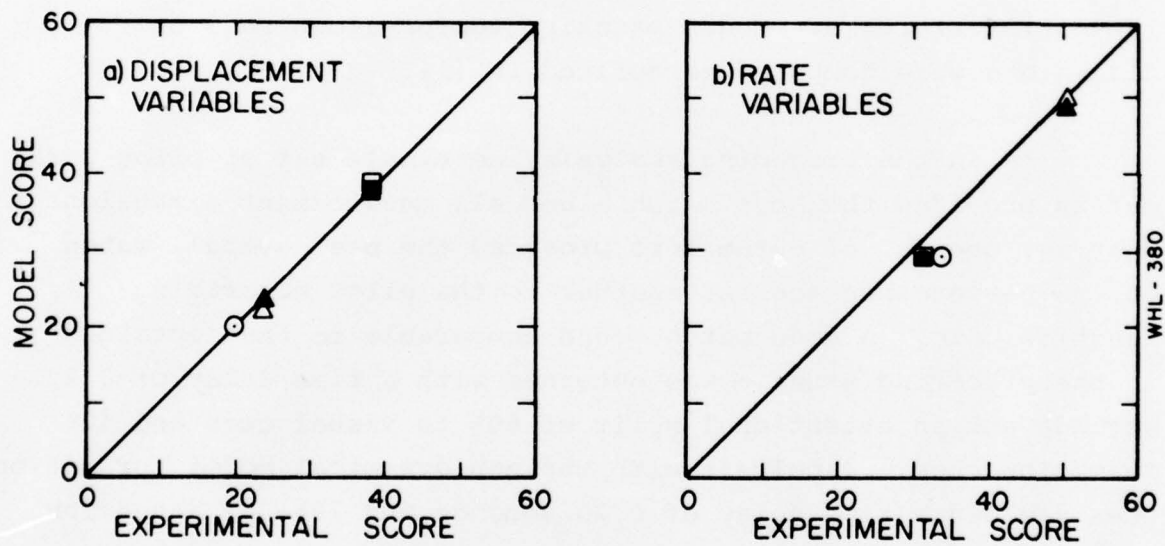
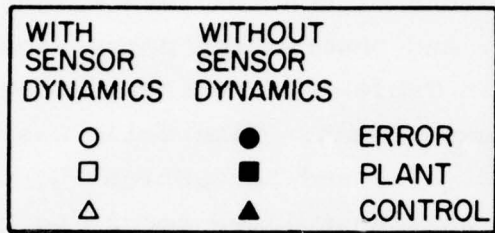


Figure 1. Effect of Sensor Dynamics on Predicted Rms Performance Scores

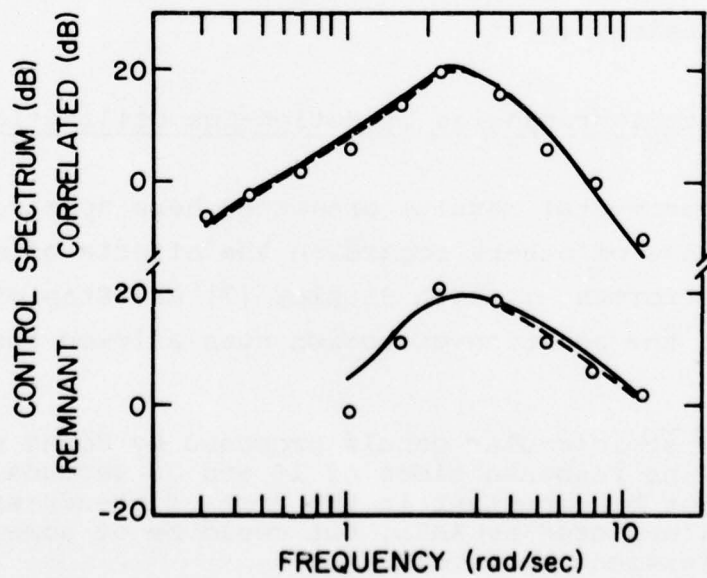
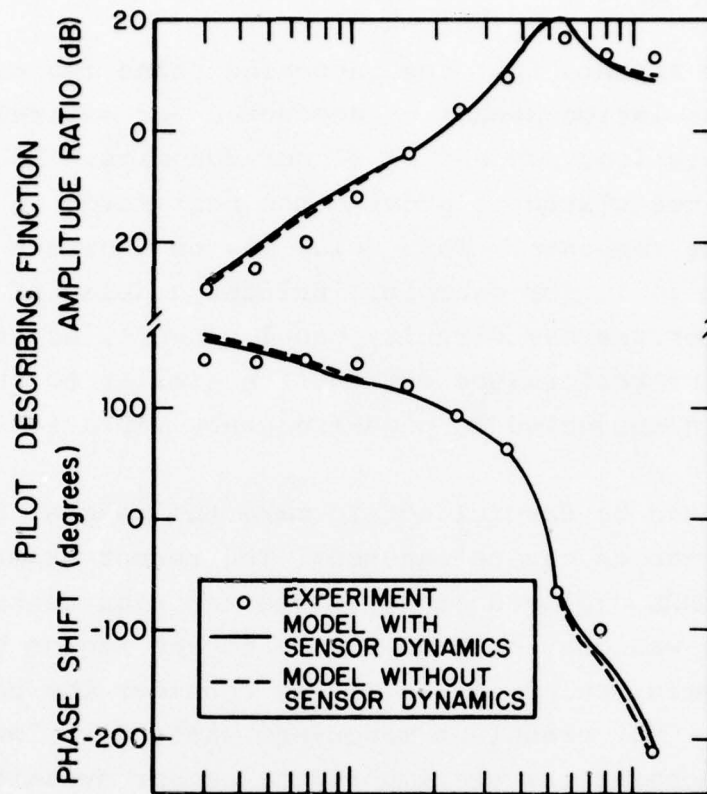


Figure 2. Effect of Sensor Dynamics on Predicted Frequency Response

It also appears that the increased phase lag associated with motion simulation cannot be accounted for entirely by bandwidth limitations imposed by sensor dynamics. Additional delay must be postulated to provide the best match to high-frequency phase response. This delay may be inherent in motion sensing (Young [4]), for example, includes a delay of 0.3 seconds in his model for the semicircular canal sensor), or it may reflect other sources of performance degradation similar to that observed when pilots are subjected to high-frequency vibration [5, 6].

One should be careful not to make the general conclusion that sensor dynamics can be ignored. The recent experiment performed at AMRL employed steady-state tracking tasks for which response power was concentrated mainly in the region of the band-pass of the semicircular canals (if we consider the canals as rate sensors). For transient maneuvers where very low frequency response characteristics are important, sensor dynamics may have to be considered. This is particularly true for situations in which the low-frequency washout characteristics of the sensors may induce illusions [3].\*

#### 2.2.2 Apparent Discrepancies in Motion-Cue Utilization

The experimental results presented here appear to conflict with the findings of others regarding the effects of motion cues on tracking performance. Both Shirley [7] and Stapleford et al. [8] concluded that the addition of motion cues allowed the pilot to

---

\*The model for semicircular canals proposed by Young contains a washout having response times of 16 and 33 seconds. These modes would not be important in the type of steady-state tracking task explored by AMRL, but could be of some consequence in certain transient maneuvers.

generate greater lead at high frequencies, thereby permitting an increase in gain-crossover frequency. Furthermore, Shirley concluded that motion cues were relatively more beneficial for tracking tasks involving low-order plants than for those involving high-order dynamics. On the contrary, the results presented above show that motion cues resulted in more high-frequency phase lag (rather than lead), no appreciable change in gain crossover, and greater relative improvement with the higher-order plant.

These apparent contradictions do not necessarily indicate that the AMRL experimental subjects used motion cues in a manner different from the subjects who participated in the studies of Shirley and of Stapleford et al. There were some important differences between the AMRL experiments and the earlier studies. Both Shirley and Stapleford et al. applied the input disturbance in such a manner that both the visual display and the motion simulator were driven by the input. (That is, the input was applied essentially in parallel with the pilot's control.) In the AMRL study, the external input was applied as a command signal; only the pilot's control signal drove the controlled plant. Thus, in the latter study, motion cues provided some inner-loop information that was not directly obtained from the visual cues. In addition, the dynamics used in Task 2 of the AMRL/BBN study were higher order than those explored in the previous studies.

In order to resolve the apparent discrepancies between the AMRL/BBN study and earlier investigations, we attempted to apply the model described above to relevant data available in the literature. After a brief review of the literature, however, we concluded that the existing data base was unsuitable for a

definitive test of the model. Specifically, we were unable to locate a study for which all of the following criteria were met:

*Complete description of the task.* In order to properly model the control task, we must know not only the vehicle dynamics and input characteristics (which are usually reported), but also display gain and stick force/displacement characteristics (which are often omitted). Knowledge of gain is needed so that we can model the effects (if any) of visual resolution limitations. Control-stick characteristics must be known so that high-frequency pilot response behavior can be properly modeled.

*Complete description of response behavior.* Published results usually include mean-squared error and sometimes pilot (or combined man-machine) describing functions. This set of measurements is not sufficient for identification of pilot-related model parameters. Pilot remnant spectra are usually required for proper identification of noise-related parameters, and having a more detailed set of performance scores (such as mean-squared control, plant, and some rate variables) is helpful.

*Analytic forcing function.* Analysis with the optimal-control pilot/vehicle model requires that the input be represented analytically as filtered white noise. This restriction provides no difficulty when the experimental input is either filtered noise or a sum of sinusoids constructed to simulate such a noise process. Studies reported in the literature, however, have tended to use a sum-of-sinusoids input constructed to simulate "rectangular-plus-shelf" type of spectrum (that is, a high-amplitude, low-bandwidth rectangular spectrum to serve as the primary input signal plus a low-amplitude, high-bandwidth

rectangular spectrum to allow measurements of pilot response at higher frequencies). Such an input is difficult to represent analytically without resorting to extremely high-order representations that substantially increase computational requirements.

Even if the above requirement had been met by the available data base, we would still have had to compare results across studies involving different subject populations and different motion amplitudes. Accordingly, we decided to conduct a small but carefully-controlled experiment to compare the use of motion cues in disturbance and command situations, as described in the remainder of this report.

### 3. DESCRIPTION OF EXPERIMENTS

In order to resolve apparent discrepancies between the results of the preceding phase of this study and those of earlier studies, and to further validate the pilot model, a set of experiments was conducted at AMRL to compare the utilization of motion cues in disturbance-regulation and target-following tasks. Pre-experimental model analysis was conducted to assure that (1) roll rates and accelerations would be above threshold detection levels but well below the limits imposed by the motion simulator, (2) the tracking input would provide a man-machine response bandwidth sufficient for analysis of pilot response behavior while providing a tracking task that was not unreasonably difficult, and (3) motion cues would have a statistically significant effect on pilot response behavior. This design procedure was successful, and experimental results were very close to those predicted a priori by the model. The design procedure has been reported in the literature [9, 10].

#### 3.1 Description of the Tasks

A Multi-Axis Tracking Simulator (MATS) was used as the controlled vehicle; only the roll-axis motion capability was used in this experiment. The simulator consisted of a single-seat cockpit with a television monitor display and side mounted force stick for vehicle control. The vehicle cockpit was light-tight to eliminate external visual cues. The roll axis system dynamics were identified and simulated on a hybrid computer. The system characteristics are presented in Table 1.

Table 1  
Multi-Axis Tracking Simulator:  
Roll-Axis Characteristics

Plant Dynamics:  $\frac{\text{PLANT}}{\text{CONTROL}} = K \frac{20}{s(s + 20)}$

Position Limit: 90 degrees

Velocity Limit: 60 degrees/second

Acceleration Limit: 100 degrees/second<sup>2</sup>

To test the capabilities of the optimal-control pilot-vehicle model, it was decided to investigate the effects of two types of tracking inputs in this experiment. One was defined as the "target" condition because vehicle motion was commanded as a result of following a target, and the other the "disturbance" condition because disturbance inputs drove the vehicle directly. Both conditions were investigated with and without the motion system on, making a total of four experimental conditions.

The block diagram for the experiment, presented in Figure 3, shows all conditions. The disturbance input was set to zero for the target condition, and the target input was set to zero for the disturbance condition.

In the target condition the task was to follow a target aircraft in the roll axis. The difference between the target roll angle and the controlled vehicle position was provided to the human operator on a 9 inch diagonal television monitor. The inside-out display consisted of a 1.25 inch long rotating line whose center was superimposed upon a stationary horizontal line as indicated in Figure 4. A 0.083 inch perpendicular line at the center of the rotating line provided upright orientation. The angle between the rotating and stationary line depicted the difference between the controlled plant roll angle and the target roll angle. The display was centered in azimuth a distance of about 20 inches from the controller's eyes. Subjects' sitting heights were such that the display was within 10 degrees of eye level of each subject.

For the disturbance conditions, the displayed error equalled the bank angle of the controlled vehicle, and the task was to null out the bank angle by keeping the controlled vehicle upright.

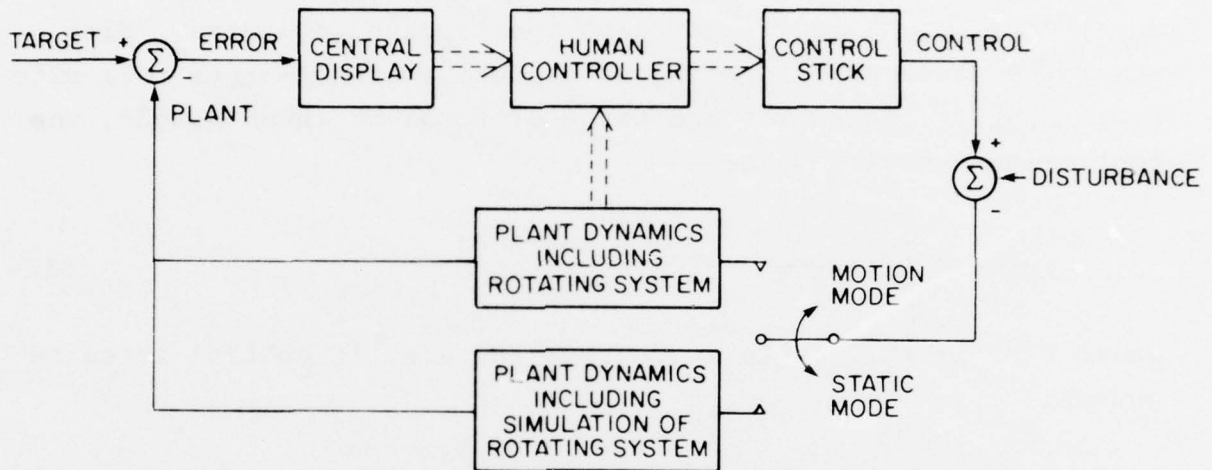


Figure 3. Block Diagram of the Tracking Task

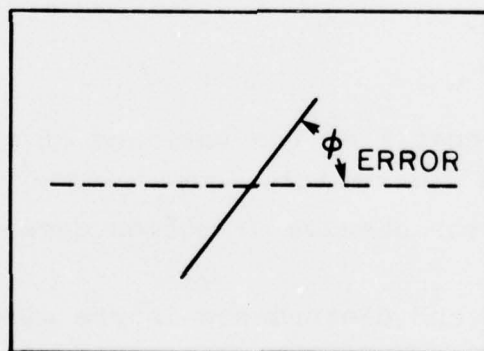


Figure 4. Sketch of the Central Display

A low-pass filter with a break frequency of 5 radians/second was added to the simulator dynamics to approximate roll-axis dynamics of high-performance fighter aircraft; in addition, recording and computational delays added an effective overall delay of about 95 milliseconds to the tracking dynamics. With the force stick gain adjusted to produce a steady-state roll rate of 10 degrees/second for one pound of force at thumb height, the controlled dynamics were:

$$\frac{P(s)}{U(s)} = \frac{10}{s} \cdot \frac{5}{s+5} \cdot \frac{20}{s+20} \cdot e^{-0.095s} \quad (3)$$

where  $P(s)$  is roll angle in degrees and  $U(s)$  is control force in pounds.

To keep RMS response rate and acceleration well below the physical limitations of the rotating simulator, as well as to encourage the test subjects (who were not trained pilots) to respond in a smooth manner, a performance criterion was defined as the weighted sum of mean-squared tracking error and mean-squared vehicle acceleration:

$$C = \sigma_e^2 + 0.1 \sigma_{\ddot{p}}^2 \quad (4)$$

where  $C$  is the total "cost,"  $\sigma_e^2$  the variance of the tracking error, and  $\sigma_{\ddot{p}}^2$  the variance of the vehicle acceleration (or acceleration of the simulated vehicle, in the absence of motion cues).

Both the target and disturbance inputs were constructed from 13 sinusoids whose amplitudes were selected to simulate random noise processes having power spectral densities of the form

$$\phi_{ii}(\omega) = \left| \frac{K}{(j\omega + \omega_i)^2} \right|^2 \quad (5)$$

where  $\omega_i$  was 1.0 rad/sec for the target input and 2.0 rad/sec for the disturbance input. Input amplitude was adjusted to provide an RMS target input of 10 degrees or an RMS disturbance input of 14 deg/sec. In order to prevent subjects from learning the input waveforms during the experiment, a random number generator was used to vary the phase relationships of the input sinusoids from one experimental trial to the next.

### 3.2 Experimental Procedure

Six healthy college students between 18 and 25 years of age were used for the experiment. Subjects tracked each condition once each day. Tracking under each condition was considered one run. Each run lasted 165 seconds and the four conditions or runs were presented in a random order each day. At the end of each run subjects were presented their three performance scores for that run: total cost  $C$ , error variance  $\sigma_e^2$  and weighted acceleration  $0.1 \sigma_p^2$ . They were instructed to minimize the total cost  $C$ . In addition, they were told that the error score was related to how much error they allowed, that the acceleration score was related to how smoothly they tracked, and that the total score was the sum of the error and acceleration scores. They were not told predicted scores, nor were they told how to divide their total score between error and acceleration. To maintain subject motivation, subjects were also made aware of each other's performance scores. Each subject wore a flight helmet with intercom capability while performing the tracking task. The subject was permitted to perform the task briefly prior to each scored run in order to adjust mentally and physically to the tracking task.

Performance scores were plotted daily in order to evaluate subject and group performance. Once the error scores indicated that the subjects had "learned" the tracking tasks for all experimental conditions, tracking was continued for another eight days and time history data was collected for subsequent analysis.

## 4. EXPERIMENTAL RESULTS

The major results of the roll-axis tracking experiment described above are summarized in this section. Appendix B contains additional, more detailed results in tabular form, and some learning data is analyzed in Appendix C. Primary data reduction and model analysis are described separately.

### 4.1 Primary Data Reduction

#### 4.1.1 Analysis Procedures

Total "cost" as defined in Equation (4) was computed for each experimental trial used for data analysis. Also computed for each trial were variance scores for tracking error, error rate, plant position (i.e., bank angle),\* plant rate, plant acceleration, control force, and control rate. To compute the variance of a rate variable, we first scaled the spectrum of the corresponding position variable by  $\omega^2$  and then integrated the modified spectrum; approximations were obtained for plant variance as described in Appendix A.

Square roots were taken of total cost and variance scores to yield rms performance measures. These measures were first averaged across replications of a given test subject for each experimental condition; the mean and standard deviation of the subject means pertaining to each experimental condition were then computed. In order to test for significant differences between motion and static conditions, paired differences were formed from corresponding subject means; these differences were subjected to a two-tailed t-test.

---

\*For disturbance-regulation tasks, tracking error and error rate were identical to plant position and plant rate.

Frequency-response analysis was similar to that employed in the preceding study [1]. The pilot describing function (specified by amplitude ratio and phase shift as functions of frequency) was computed by dividing the Fourier transform of the pilot's control response by the transform of the tracking error. For situations in which the rotating simulator was operative, this transfer function reflects the combined effects of visual and motion cues on pilot response. In all cases, the measured phase shift was corrected to account for phase lags introduced by the simulation and data-recording procedures as described in Appendix A.

Estimates of "pilot remnant" were obtained by partitioning the spectrum of each control response into input-correlated and remnant-related (i.e., stochastic) components and, at each measurement frequency, obtaining the ratio of remnant-related to input-correlated power. As was done with other performance measures, these ratios were averaged across replications of a given subject and then across subjects. T-tests were performed on all frequency response measures in the manner described above.

The data base subjected to detailed analysis consisted of the last eight trials per subject per condition, with the exception that trials yielding atypical performance were excluded. "Atypical" trials were identified as follows:

1. Means and variances for all performance metrics were computed from the last eight runs of a given subject performing a given task.

2. Sets of performance metrics were constructed of like quantities. That is, rms performance scores consisted of one set, measures of pilot amplitude ratio another, etc.
3. Tests for atypicality were performed individually on each measurement set. Trials which yielded a measurement set that was, on the average, two or more standard deviations away from mean performance were excluded from the data base.

This test resulted in the exclusion of only three (out of a total of 192) trials. A similar test was performed on the subject means to determine if the performance of any subject was atypical of the group. No "atypical" subjects were found by this definition.

#### 4.1.2 Results

Variables for which rms performance scores were computed, their units, and their symbolic notation are shown in Table 2. Average rms performance scores are shown in Figure 5. For ease of comparison with other performance metrics, the square root of the "cost" defined in Equation (1) is shown, and various rms scores have been scaled so that all scores may be shown on the same ordinate scale. Significant static-motion differences are indicated by the arrows, where the coding of the arrow indicates the significance level as defined in Table 3. Mean performance scores and standard deviations of subject means are given in Appendix B, Tables B-1 and B-2.

Table 2  
Tracking Variables Analyzed

Variable	Symbol	Units
Total Performance Cost	C	---
Tracking Error	e	degrees
Tracking Error Rate	$\dot{e}$	degrees/second
Plant Position	p	degrees
Plant Rate	$\dot{p}$	degrees/second
Plant Acceleration	$\ddot{p}$	degrees/second <sup>2</sup>
Control Force	u	pounds
Control Rate	$\dot{u}$	pounds/second

Table 3  
Coding for Significance Level

Symbol	Alpha Level of Significance
↓	0.05
‡	0.01
‡‡	0.001

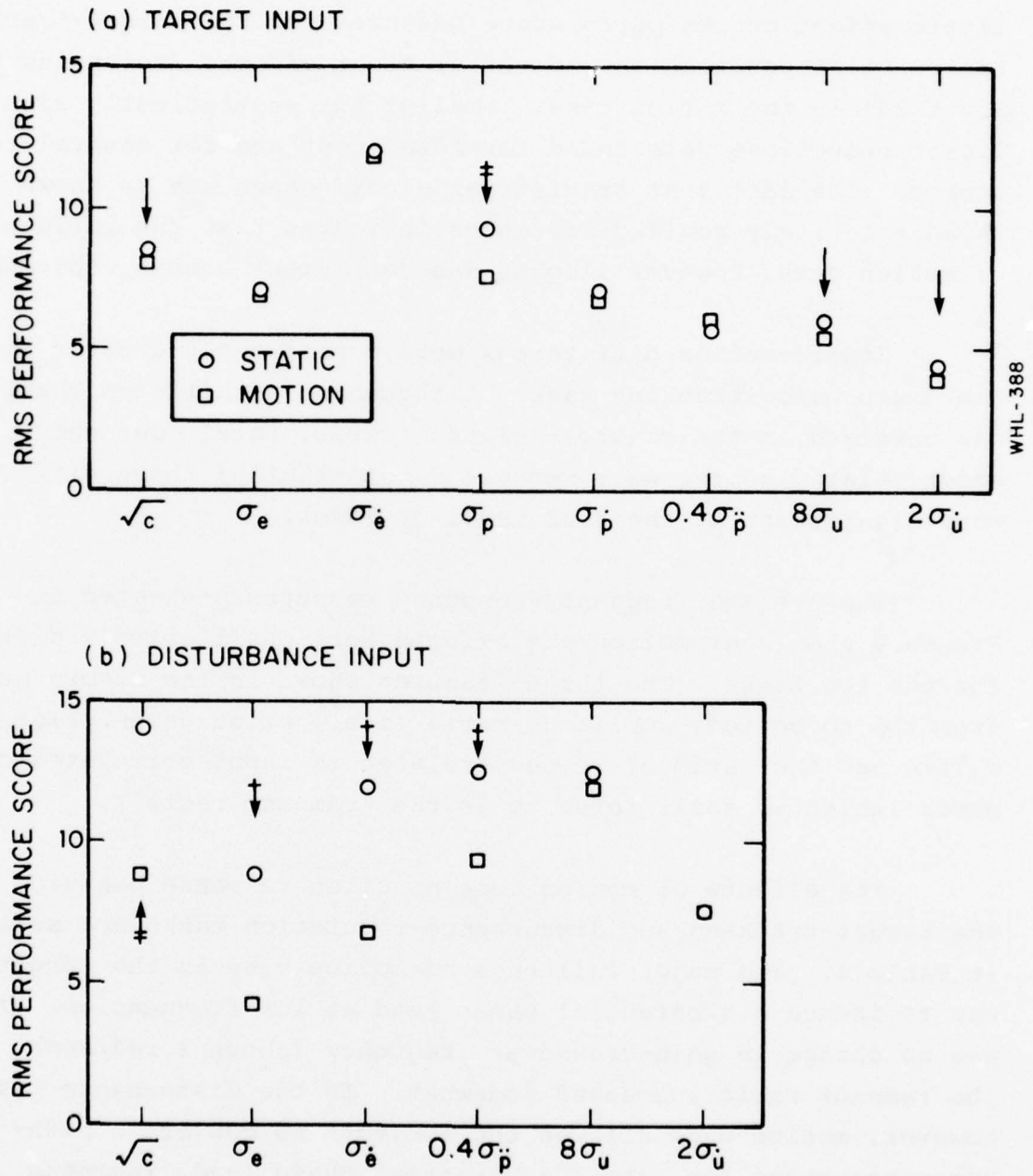


Figure 5. Effect of Motion Cues on Rms Performance Scores  
Average of 6 subjects.

Figure 5 shows that the availability of motion cues had little effect on rms performance measures for the target-tracking task. Plant position showed the greatest effect, decreasing by about 20% in the motion case. Smaller but statistically significant reductions were found for total cost and for control-related scores. The fact that statistical significance can be shown for these relatively small differences indicates that the influence of motion cues, however slight, was consistent across subjects.

Static-motion differences were considerably greater for the disturbance-tracking task. Although no significant change was observed in the control-related scores, total cost and error-related scores were reduced substantially; these differences were significant at the 0.01 level or lower.

The average frequency-response measures presented in Figure 6 show that motion-cue effects were qualitatively different for the two tasks. The three measures shown in the figure are, from top to bottom, amplitude ratio (i.e., pilot gain), pilot phase shift, and the ratio of remnant-related to input-correlated control power (which we shall refer to as the "remnant ratio").

The effects of motion cues on pilot response behavior for the target-tracking and disturbance-regulation tasks are summarized in Table 4. The major influence of motion cues in the target task was to induce a substantial phase lead at low frequencies. There was no change in gain-crossover frequency (about 1 rad/sec), and the remnant ratio increased somewhat. In the disturbance task, however, motion cues allowed the subjects to convert a high-frequency phase lag into a substantial phase lead, increase amplitude ratio at low and mid frequencies, and thereby increase gain-crossover frequency from about 1.5 rad/sec to around 3.5 rad/sec.

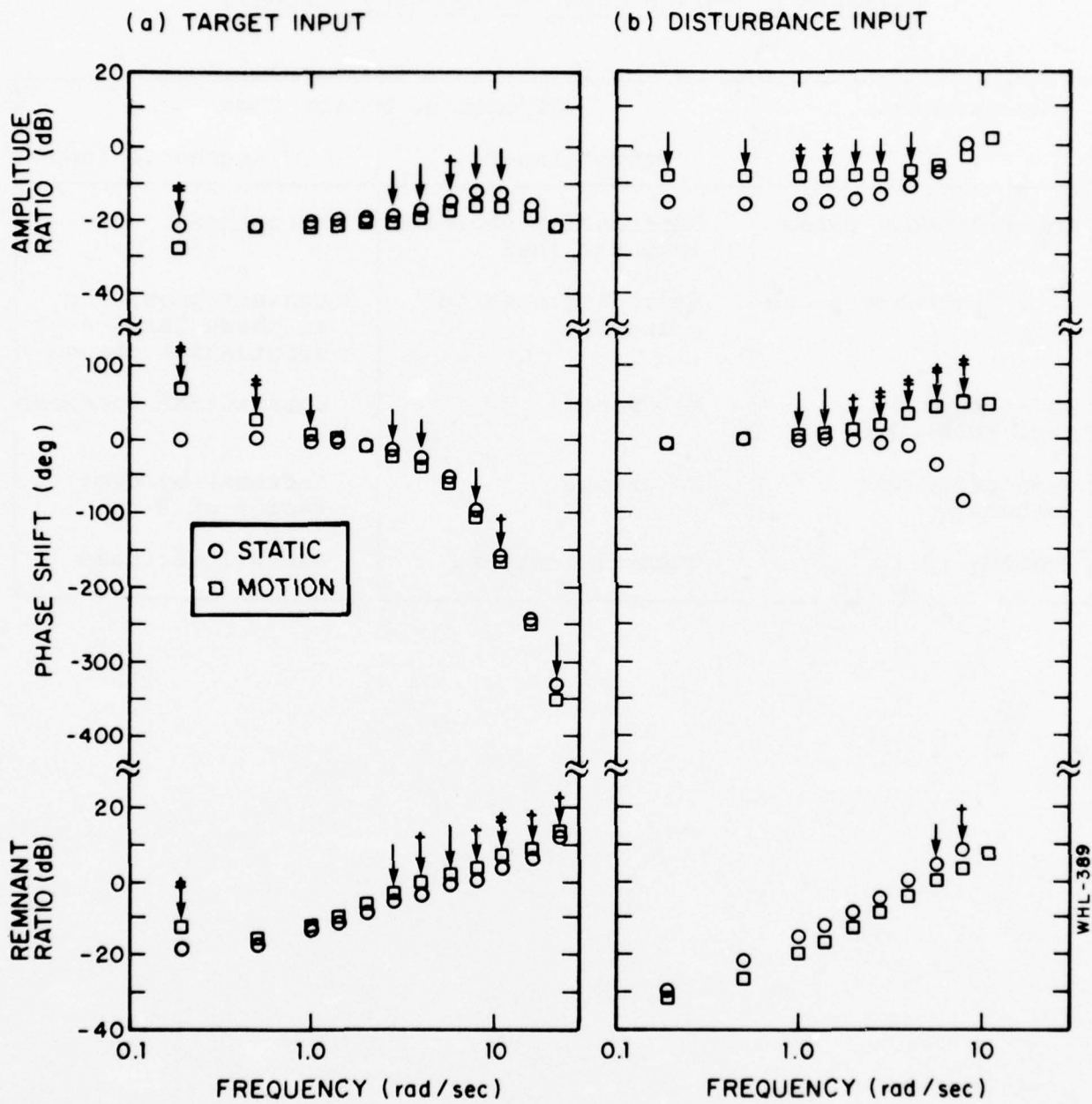


Figure 6. Effect of Motion Cues on Pilot Frequency Response  
 0 dB represents 1 pound control force per degree roll for the amplitude ratio and unity (dimensionless) for the remnant ratio.  
 Average of 6 subjects.

Table 4

Effects of Motion Cues on Frequency Response

Measurement	Effects of Motion Cues	
	Target Input	Disturbance Input
Low-frequency phase	Substantial increase in phase lead	No change
High-frequency phase	Small increase in phase lag	Convert phase lag to phase lead, a substantial change
Low-frequency amplitude-ratio	No change	Substantial increase
Gain-crossover frequency	No change	Increase by over factor of 2
Remnant ratio	Overall increase	Overall decrease

Although motion cues allowed the remnant ratio to decrease at all frequencies for this task, static/motion differences were largely not statistically significant.

During the course of this analysis we addressed the question of whether or not the average pilot response characteristics shown in Figure 6 were typical of the response characteristics of individual subjects. That is, we wanted to ascertain that important response characteristics were not obscured by the averaging process. Accordingly, the procedure for eliminating atypical performance described in Section 4.1.1 was applied to subject means to successively eliminate all but one subject per experimental condition.

Figure 7 compares the responses of typical subjects to the average response of all six subjects for the static and motion conditions in the disturbance-regulation task. Typical and average responses very nearly coincided for the static condition. The correspondence between typical and average response was also high for the motion condition, with only small differences in overall amplitude of response. Thus, we are justified in averaging these response measures across subjects.

#### 4.1.3 Discussion of Results

The results obtained in this experiment agree qualitatively with results obtained previously in similar tracking situations. The effects of motion cues in the target-tracking task are similar to those obtained in the preceding AMRL experimental study for "Task 1" (the less severe of the two tasks studied in that program). In both cases, motion cues allowed an increase in low-frequency phase shift that was unaccompanied by any substantial improvement in tracking performance.

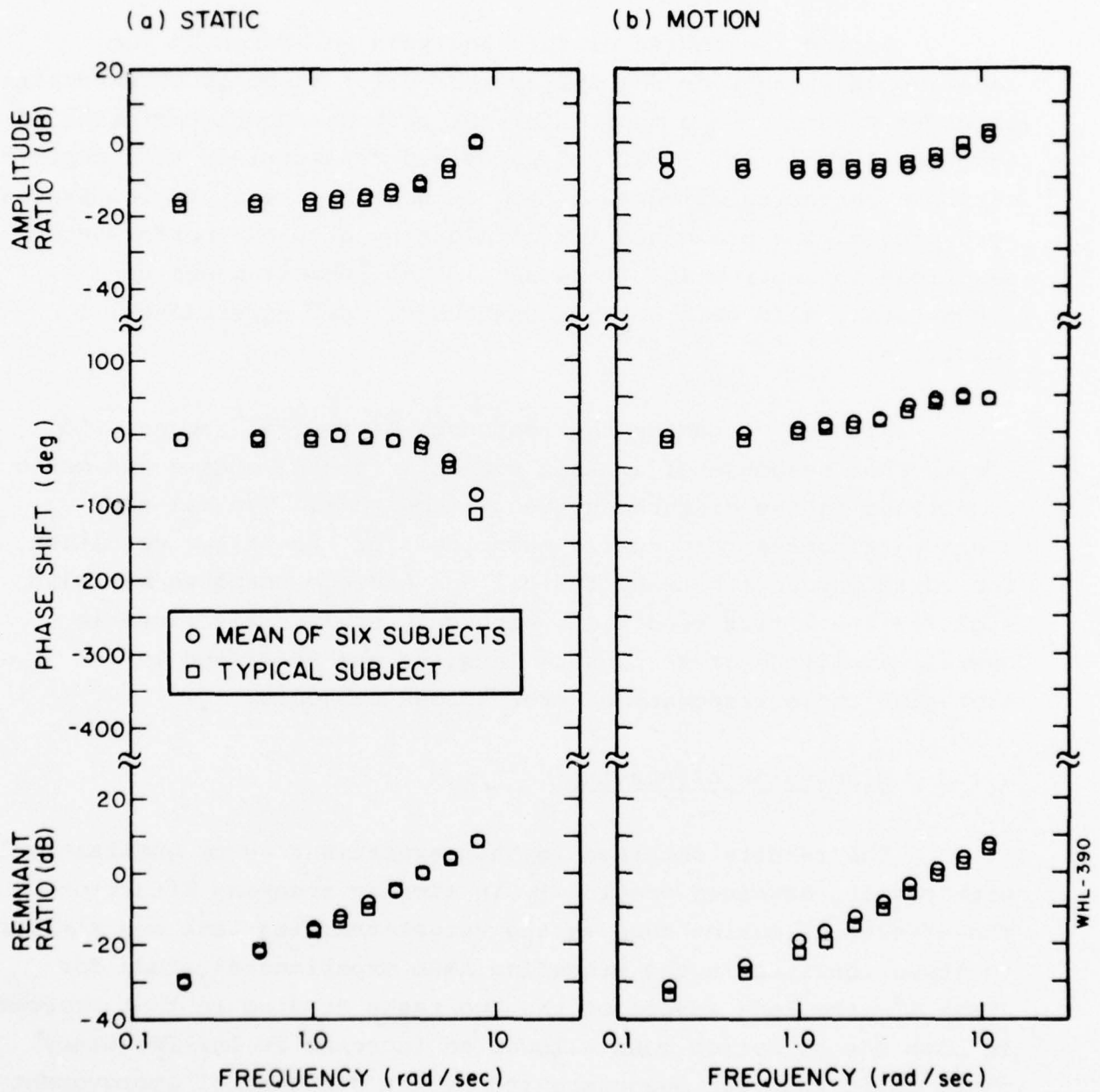


Figure 7. Comparison of Typical and Mean Responses

Similarly, the effects of motion cues observed in the disturbance-regulation task agree with the effects reported by other researchers. As noted in Chapter 2, earlier investigators reported that moving-base simulation allowed the pilot to reduce high-frequency phase lag and to increase gain-crossover frequency and thereby, in many cases, lower his error score.

Motion/static performance differences were enhanced somewhat by the time delays introduced by the data-recording and computational algorithms. These delays influenced only the visual cues provided to the pilot; the motion cues were provided by the moving-base simulator. Thus, motion cues provided a double benefit to the pilot; information was obtained via motion sensors in advance of information obtained visually, and, as we infer from the model analysis described below, vehicle acceleration and possibly rate-of-change of acceleration were also sensed.

It is clear from the results of this experiment that the effects of motion cues on pilot response cannot be generalized in terms of classical response measures. We have shown that the effects of motion cues on rms performance scores, pilot describing function, and pilot remnant can all differ qualitatively from one control situation to the next.\* Some form of generalization is needed, nevertheless, if we are to extrapolate the results of these and earlier experiments to other control tasks of interest. That is, we need a model which accounts for the interaction between available motion cues and pilot response in terms that are essentially independent of the details of the control task. Such a model is discussed below.

---

\*Relative effects of motion cues are affected not only by the type of external input, as demonstrated here; pre-experimental model analysis indicated that input bandwidth and performance criterion would also influence motion/static differences in response behavior.

## 4.2 Model Analysis

### 4.2.1 Analysis Procedure

The revised optimal-control pilot/vehicle model developed in the preceding phase of this study was applied to the results of the experiment described above. This model is described by Levison, Baron, and Junker [1].

The treatment of motion cues was similar to that of the preceding study in that the presence or absence of motion cues was represented by an appropriate definition of the sensory variables assumed to be available to the pilot. A three-element "display vector" consisting of tracking error, error rate, and (in one instance) error acceleration was used to model static-mode tracking. To model pilot response in moving-base tasks, we simply expanded this display vector to include position, rate, acceleration, and acceleration-rate of the vehicle; no other model parameters were changed to account for motion/static differences. Model runs were also obtained which included the effects of dynamic response properties of vestibular motion sensors. System equations of motion used in the model analysis are given in Appendix C.

The scheme for identifying model parameters was similar to that employed in the preceding study program. Parameter values were sought that would simultaneously provide a good match to performance scores, describing function, and remnant ratio. A multi-dimensional "matching error" was defined, with the dimensions being (1) rms performance, (2) amplitude ratio, (3) phase shift, (4) and remnant ratio. Matching error was defined in such a way that a score of unity was obtained whenever model predictions

differed on the average from experimental measurements by one standard deviation. Additional details concerning the computation of matching error are found in [1].

As in the preceding study, the primary goal of model analysis was to determine a straightforward and reliable procedure for predicting the effects of motion cues in a variety of control tasks. Therefore, we attempted to account for performance on all four tasks with the fewest variations in parameter values. We did not allow all parameters to vary in order to obtain the best match in each condition; rather, variations were made in only those parameters that could reasonably be expected to relate to the kind and quality of information provided to the pilot.

#### 4.2.2 Primary Results of Model Analysis

Attentional parameters were the only model parameters that were varied across experimental conditions; all other parameter values were held fixed. Numerical values for these parameters, shown in Table 5, were obtained as follows:

*Control-Rate Cost Coefficient.* Based on previous studies of single-variable laboratory tracking tasks, the control-rate cost coefficient was adjusted to provide a "motor time constant" of 0.1 second.

*Acceleration Cost Coefficient.* In accordance with instructions given to the subjects, we initially attempted to match experimental results with an acceleration cost coefficient of 0.1 seconds. A somewhat better match was obtained with a coefficient of 0.05, however, and this latter value was adopted for the remainder of the analysis.

Table 5

Values for Pilot-Related Model Parameters

## a. Invariant Parameters

Control-rate cost coefficient	1.0
Motor time constant	0.1 seconds
Acceleration cost coefficient	0.05
Time delay	0.22 seconds
Driving motor noise/signal ratio	(negligible)
Pseudo motor noise/signal ratio	-30 dB
Observation noise ratio for "Full Attention"	-20 dB
Perceptual thresholds, error rate, visual	3.2 deg/sec
Perceptual Thresholds, all other variables	(negligible)

## b. Attentional Allocation

Perceptual Mode	Perceptual Variable	Tracking Task			
		Target Static	Input Motion	Disturbance Static	Input Motion
Visual	error	1	0.95	1	0.1
	error rate	1	0.95	1	0.1
	error acceleration	---	---	0.05	0
Motion	plant	0	0.05	0	0.9
	plant rate	0	0.05	0	0.9
	plant acceleration	0	0.05	0	0.9
	plant acceleration rate	0	0.05	0	0.9

*Time Delay.* A time delay of 0.22 seconds provided the best match across conditions.

*Motor Noise/Signal Ratios.* On the basis of previous analysis, the "driving" motor noise/signal ratio was made negligibly small; a "pseudo" noise/signal ratio of -30 dB gave a reasonably good match to low-frequency phase shift (See Levison, Baron, and Junker for a discussion of the motor noise aspect of the pilot model.)

*Observation Noise/Signal Ratio.* On the basis of previous studies, an observation noise/signal ratio of -20 dB was adopted.

*Perceptual Thresholds.* Because vehicle roll rates and accelerations were large compared to published detection thresholds for these variables, thresholds for motion-related variables were set to zero. A good match to the data was obtained with thresholds of 0 degrees and 3.2 deg/sec associated with visually-obtained error and error rate. As discussed in Appendix C, these values were smaller than those obtained from preliminary display analysis.

*Attentional Variables.* With the exception of visually-obtained error acceleration, attention was assumed to be shared between visual display variables as a group and motion variables as a group, and there was assumed to be no interference among perceptual quantities within a sensory mode. The absence of motion-related information in a tracking task was modeled as zero attention (i.e., extremely large observation noise) on motion variables and unity attention on visual variables. The attentional allocations between visual and motion cues shown in Table 5 provided the best match to the data.

Figure 8 shows that the model accurately reflected the influence of both the nature of the external input and the presence or absence of motion cues. Of the 28 performance scores predicted by the model, all but three were within 10 percent of corresponding experimental measures; and in only one of these cases did the model score fail to be within one standard deviation of the experimental mean.

As shown in Figure 9, model outputs agreed quite well with experimental frequency-response measures, and major trends in the data were predicted. Specifically, inclusion of motion-related sensory information caused the model to predict an increase in low-frequency phase shift for the target task. For the disturbance task, the model correctly predicted large increases in low-frequency gain and high-frequency phase lead. The model also predicted an overall decrease in remnant ratio for this task.

It is worthwhile to re-emphasize that the effects of motion cues have been accounted for solely by changes in model parameters related to the information availability and quality; other parameters have been kept fixed for the four experimental conditions.

Values for two of the parameters - cost-of-acceleration and time delay - were somewhat different from those initially expected. The acceleration cost coefficient that provided the best fit to the data was half that used in computing the total performance cost during the experiments. In order to estimate the subject's ability to detect differences between subjective and objective cost criteria, model results were obtained for acceleration cost coefficients of 0.05, 0.1, and 0.2. The

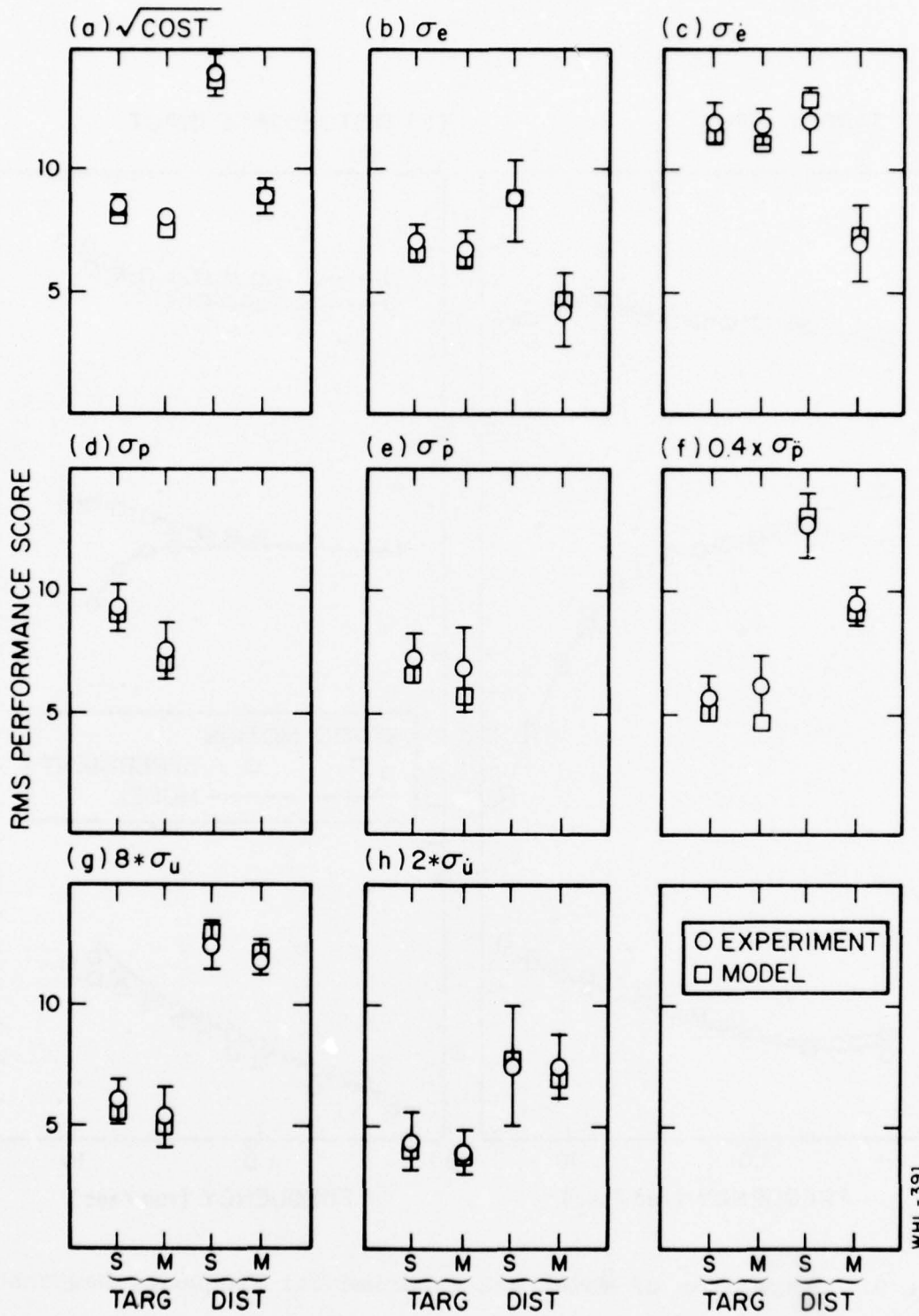


Figure 8. Comparison of Model and Experimental Performance Scores  
 S = static condition, M = motion condition.  
 Average of 6 subjects.

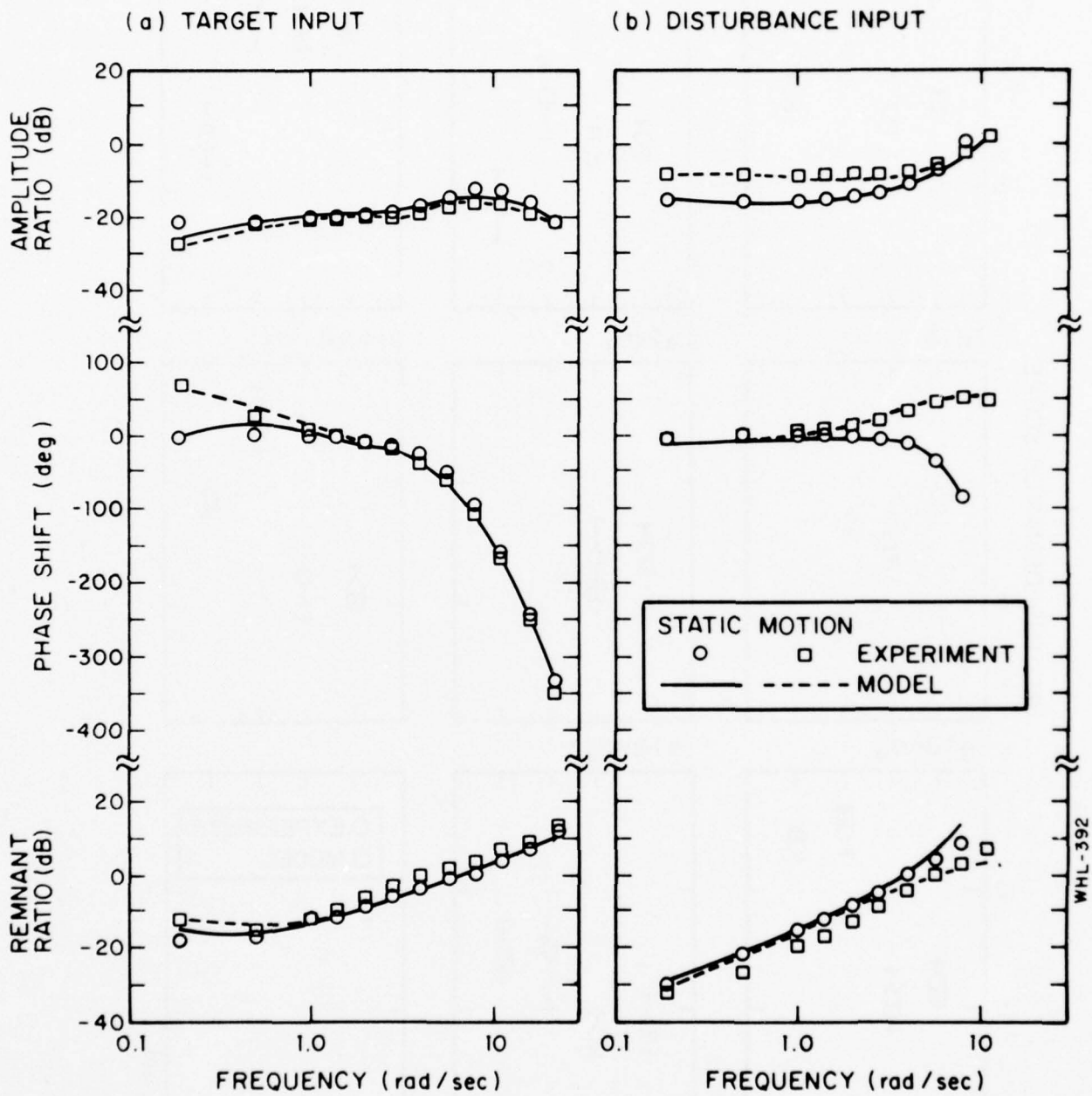


Figure 9. Comparison of Model and Experimental Frequency Response  
 Average of 6 subjects.

weighting on control rate was varied to maintain a motor time constant of 0.1 seconds, and other model parameters were kept fixed at values shown in Table 5. This sensitivity study was performed for the target-tracking task, visual inputs only.

Total cost, computed as defined in Equation (4), varied by less than 5% for the range of cost coefficients explored (a factor of 4). Therefore, the subjects had no clear indication that their performance was not optimal (as defined by the objective cost criterion). In effect, they achieved a slight reduction in error score by allowing a slight increase in acceleration score with no perceptible effect on overall performance cost.

The best-fitting time delay of 0.22 seconds was outside the range (0.15 to 0.20 seconds) usually found in laboratory tracking tasks employing plant dynamics of reasonable bandwidth. Again, the pilot may have operated with this time delay because of the relative insensitivity of performance to this parameter. Model analysis of the target/visual task showed that the total cost associated with a time delay of 0.22 seconds would be only about 6% greater than the cost achieved with a time delay of 0.15 seconds. The lack of sensitivity of performance to time delay reflects, at least in part, the restraining influence of the acceleration cost on response bandwidth. That is, the imposition of a cost on acceleration imposes a reduction in pilot gain, which in turn reduces man-machine system bandwidth. This factor would tend to mask the effects of moderate increases in pilot time delay.

The principal effect of including a low level of attention to visually-obtained error acceleration in the disturbance/static condition is to improve the match to high-frequency remnant. This result is consistent with an earlier study by Levison of the effects of display bandwidth on visual-only tracking [11]. Overall tracking performance, however, is little influenced by the availability of error acceleration information at the level indicated in Table 5. Removal of this quantity from the display vector causes an increase in rms tracking error of less than 3 percent, and other scores change by even smaller amounts.

#### 4.2.3 Alternate Hypotheses

As in the preceding study, we have assumed that there is interference (i.e., attention-sharing requirements) between visual inputs as a group and motion variables as a group. We have also introduced a new hypothesis: that acceleration rate ("jerk") is one of the cues provided to the subject in the moving-base simulation.

Average matching errors are shown in Figure 10 for the various hypotheses. Also shown are the matching errors for the individual measurement dimensions (rms performance scores, pilot gain, pilot phase shift, and remnant ratio). The assumption of interference provided somewhat lower matching errors for the target-following results - essentially no difference for the disturbance-regulation results. Thus, we cannot claim to have proven the existence of interference, only that such a hypothesis is consistent with the data.

Inclusion of jerk in the display vector has no effect on model predictions for the target-following task; thus, this hypothesis is not shown in Figure 10a. Figure 10b shows, however,

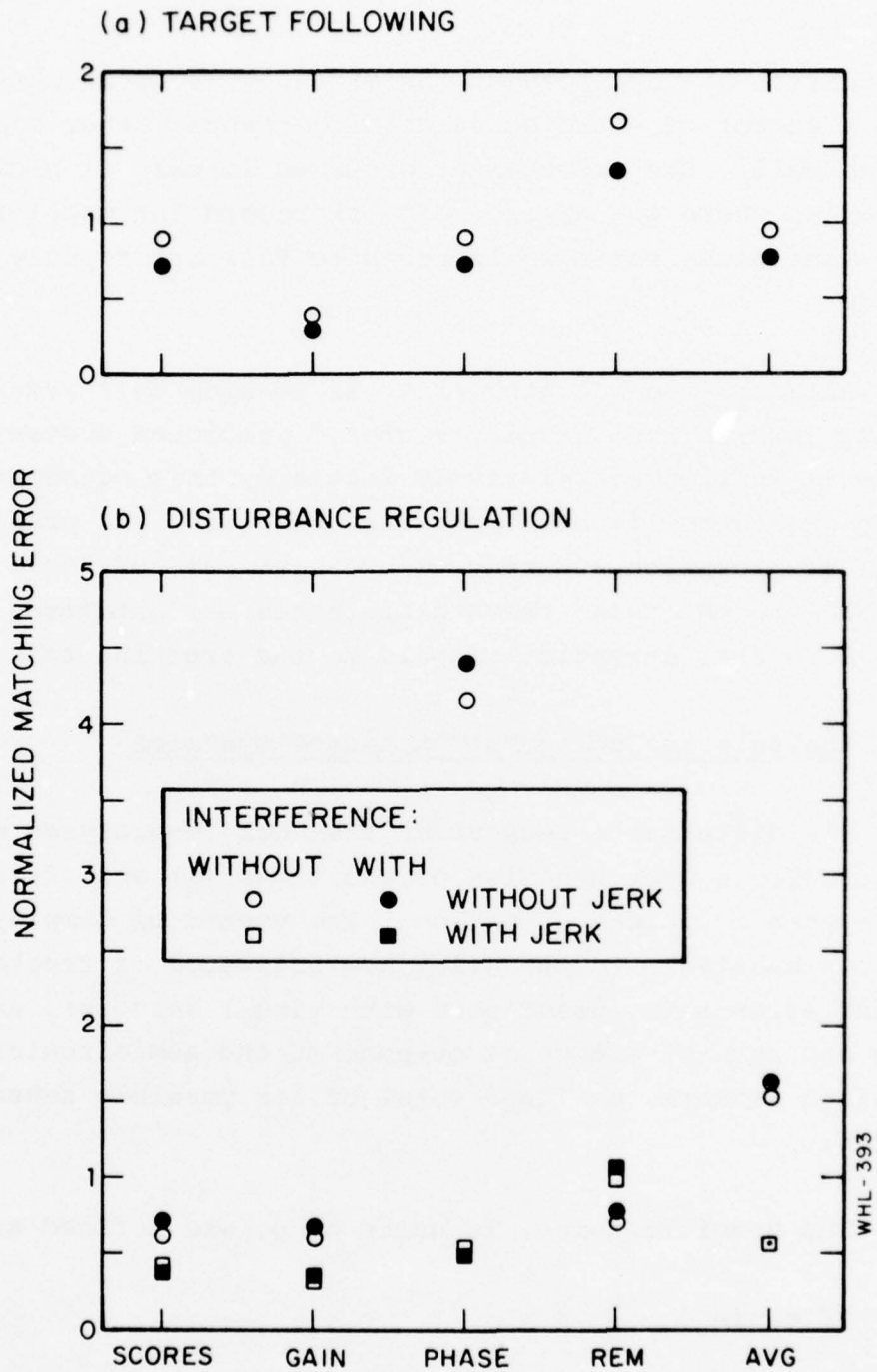


Figure 10. Matching Errors for Various Hypotheses

that inclusion of jerk reduced the matching error on phase shift by over a factor of 4 and substantially reduced other component errors as well. The improvement occurred largely at high-frequencies, where the absence of jerk caused the model to predict that phase shift would begin to fall off rapidly above 8 rad/sec.

Although the matching error is considerably reduced by including jerk in the "display vector," predicted system performance is influenced relatively little by this consideration. As shown in Figure 11, both predicted rms error and predicted rms roll acceleration are reduced by about 10% for "full attention"\* to the task; these differences are predicted to disappear as less attention is paid to the tracking task.

#### 4.2.4 Analysis Including Motion Sensor Dynamics

The disturbance-regulation task was re-analyzed with the vestibular sensor dynamics of equations (1) and (2) added to the system equations of motion. The vector of displayed quantities available to the pilot now consisted of tracking error and error-rate (associated with visual sensors), and the outputs and rate-of-change of outputs of the semicircular canal and otolith sensors, making a total of six possible sensory variables.

The specific force, in units of g, was defined as

$$SF = \sin \phi - \frac{R}{g} \ddot{\phi} \quad (6)$$

where  $\phi$  is the bank angle of the motion simulator, R is the

\*"Full attention" corresponds to a base observation noise/signal ratio of 20 dB - a level that pilots have been found to adopt for most laboratory tracking tasks in which they are motivated to perform well.

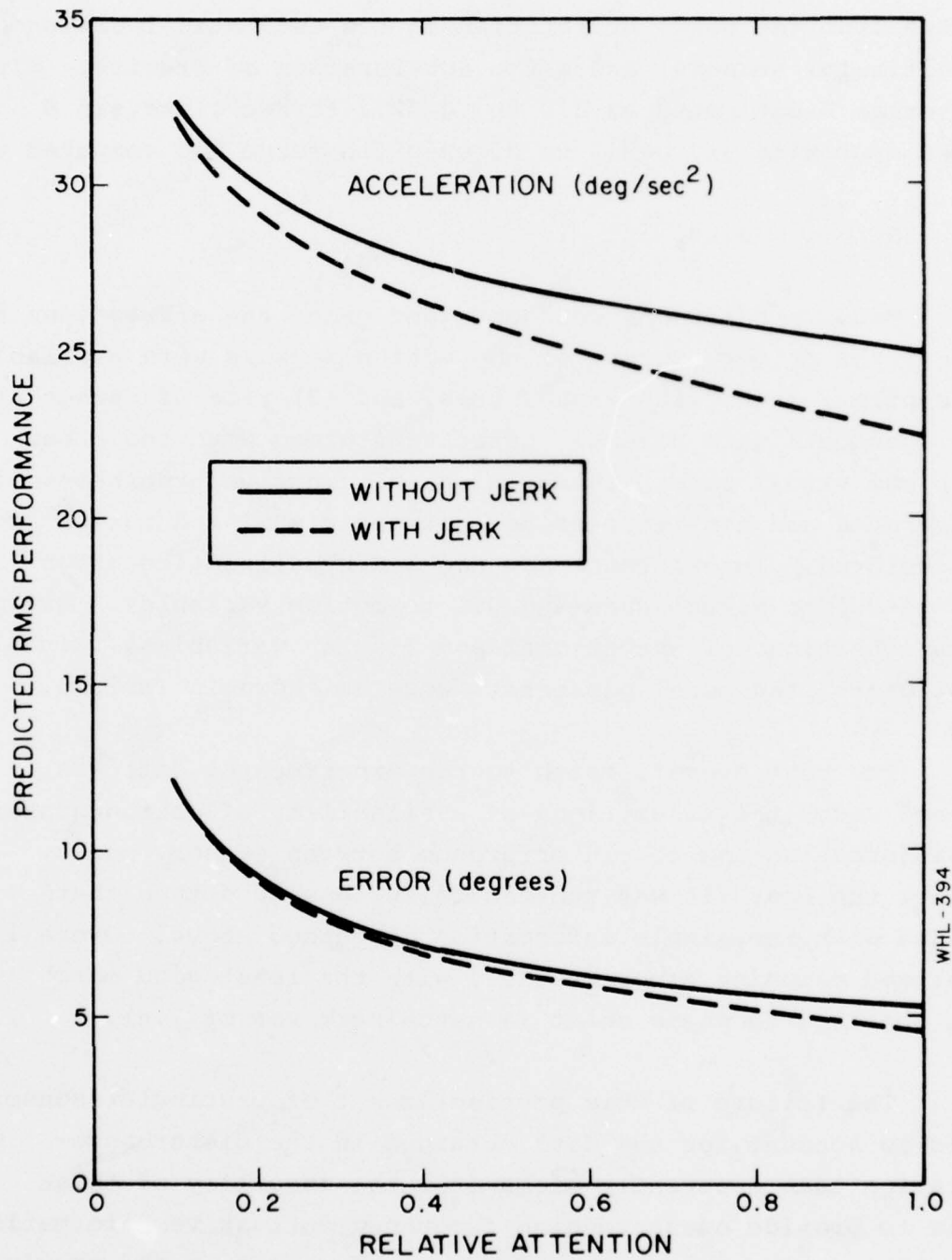


Figure 11. Effect of Acceleration-Rate Perception on Predicted Performance

distance from the point of rotation to the estimated location of the vestibular sensors, and  $g$  the acceleration of gravity. With the average  $R$  estimated as 3.0 ft,  $g=32.2 \text{ ft/sec}^2$ , and  $\sin \theta$  assumed approximately equal to  $\theta$ , specific force was computed as

$$SF = \phi - 0.093 \ddot{\phi} \quad (7)$$

Model predictions were obtained under the assumptions that (1) only the primary output of the motion sensors were available to the pilot, along with visual cues, and (2) rate-of-change of sensors outputs were directly perceived, along with the other motion and visual cues. In addition, alternative hypotheses of interference and non-interference between visual and motion cues were explored. Interference was modeled by allocating attentions of 0.1 to visual cues and 0.9 to motion variables. Except for manipulations of attentional and display variables, values for pilot-related model parameters were as shown in Table 5.

The best overall match to the experimental data was obtained under the assumptions of availability of motion-sensor-rate information and non-interference between sensory modes. However, the best fit was substantially less good than that obtained with the simple information discussed above. Overall normalized matching error was 3.1, with the least good match being obtained to phase shift (a matching error of 7.6).

The failure of this particular set of vestibular-sensor models to account for the data obtained in the disturbance-regulation task apparently stems from the inability of these models to provide adequate high-frequency derivative information. (Note that in the target-tracking tasks explored in the previous study phase, *low-frequency* lead information was needed.) Even if

sensor-rate information is assumed to be directly perceived by the pilot, the following shortcomings are encountered: (1) acceleration information available from the semicircular canals is filtered at high frequencies; (2) acceleration information from the otoliths is confounded with position information; and (3) jerk information is not directly available to the pilot.

The vestibular models recently used by Curry, Hoffman, and Young [12] appeared to provide the desired high-frequency information and model results were obtained with this model set. As described in Appendix C, system equations were augmented by the following model elements:

$$Y_s = \frac{188 (.02s + 1)}{(18s + 1) (30s + 1)} \ddot{\phi} \quad (8)$$

$$Y_o = \frac{91.1(s + .0988)}{(s + 0.2)} SF \quad (9)$$

where  $Y_s$  and  $Y_o$  are outputs proportional to the sensations yielded by the semicircular canals and otoliths, respectively.\* In addition, the rate quantities  $\dot{Y}_s$  and  $\dot{Y}_o$  were included as outputs available to the pilot in some of the model runs.

Model analysis was conducted as described above. Again, the best match to experimental data was obtained with the assumption that motion-sensor-rate information was used and that there was no interference between visual and motion cues. The match

---

\*The models used by Hoffman et al. also included residual noise terms to reflect sensory resolution limitations. Because vehicle accelerations encountered in AMRL experiments were large compared to published sensory thresholds, these noise terms were neglected in the analysis.

to the data, however, was much closer than with the previously explored vestibular models. Average normalized matching error was about 0.77 with a maximum component error (on phase) of about 1.3. Performance scores were closely matched as well: predicted rms scores differed from experimental scores by less than 3% average absolute error in amplitude ratio was about 0.3 dB, average error in phase less than 4 degrees, and average error in remnant ratio was about 0.4 dB.

As was the case with the results of the previous study, we again find that models of vestibular dynamics are consistent with results obtained experimentally (provided we select the right models), but overall modeling accuracy is not enhanced by the consideration of such motion-sensor models. Thus, a straightforward informational analysis would appear to be adequate for predicting the effects of motion cues on tracking performance and pilot response for the types of control tasks considered in this study.

On the basis of results explored so far under this contract, the inclusion of vestibular system dynamics in the pilot/vehicle model appears to impose an unnecessary computational burden. This may be partly because of the existence of potential sources of motion information (e.g., tactile and kinesthetic cues) not accounted for by models of vestibular sensory apparatus. Also, as noted earlier, this analysis has been devoted to steady-state tracking tasks in which response power has largely been within the passband of the vestibular sensors; thus, dynamic response characteristics of the latter would not play an important role in determining pilot response. For transient maneuvers, on the other hand, such dynamics could well be important.

#### 4.2.5 Reanalysis with Typical Pilot Parameters

By allowing nearly all pilot-related model parameters to vary from one study to the next, we have been able to obtain close agreement between model and experimental results for all tasks explored in the two studies completed under this contract. Many of these parameter differences have been attributed to the relative insensitivity of overall system performance to such parameter values.

If the model is to be used as a *predictive* rather than as a *diagnostic* tool, it is important that one be able to predict the effects of task variables on system performance using a single set of typical pilot parameter values. Because there generally exists a range of pilot response behavior that gives near-optimal system performance in a typical control situation, one would not expect such a procedure to yield accurate predictions of all response metrics. Nevertheless, one would expect that important trends in system behavior would be revealed.

To test the predictive capability of the model, a comparison was obtained between measured and predicted rms tracking error for all eight tasks explored under this contract, using a set of "typical" pilot parameter values. These values were chosen largely on the basis of previous laboratory studies and are not necessarily those that would provide the best overall fit to the data base. The following parameter values were used:

*Cost Functional.* Cost functionals were  $J = \sigma_e^2 + G \sigma_{\dot{u}}^2$  for the tasks explored in the previous study phase [1] and  $J = \sigma_e^2 + 0.1 \sigma_p^2 + G \sigma_{\dot{u}}^2$  for the tasks described in this report. The coefficient G was chosen to provide a motor time constant of 0.1 seconds in all cases.

*Time Delay.* A pilot time delay of 0.2 seconds was assumed.

*Perceptual Thresholds.* Thresholds of 1.6 degrees for visual perception of tracking error and 6.4 degrees/second for visual perception of error rate were calculated as described in Appendix C. Because of the large vehicle motions, thresholds for motion-derived perceptions were assumed negligible.

*Motor Noise/Signal Ratios.* Driving motor/noise signal ratio was negligibly small; pseudo noise/signal ratio was set at -35 dB.

*Observation Noise/Signal Ratio.* A value of -20 dB was used.

As shown in Figure 12, model predictions correlated well with experimental measures. ("Year 1" and "Year 2" refer to the studies described in [1] and in this report, respectively.) All significant trends related to task configuration and availability of motion cues were predicted. Furthermore, individual scores were predicted, on the average, to within 15%.

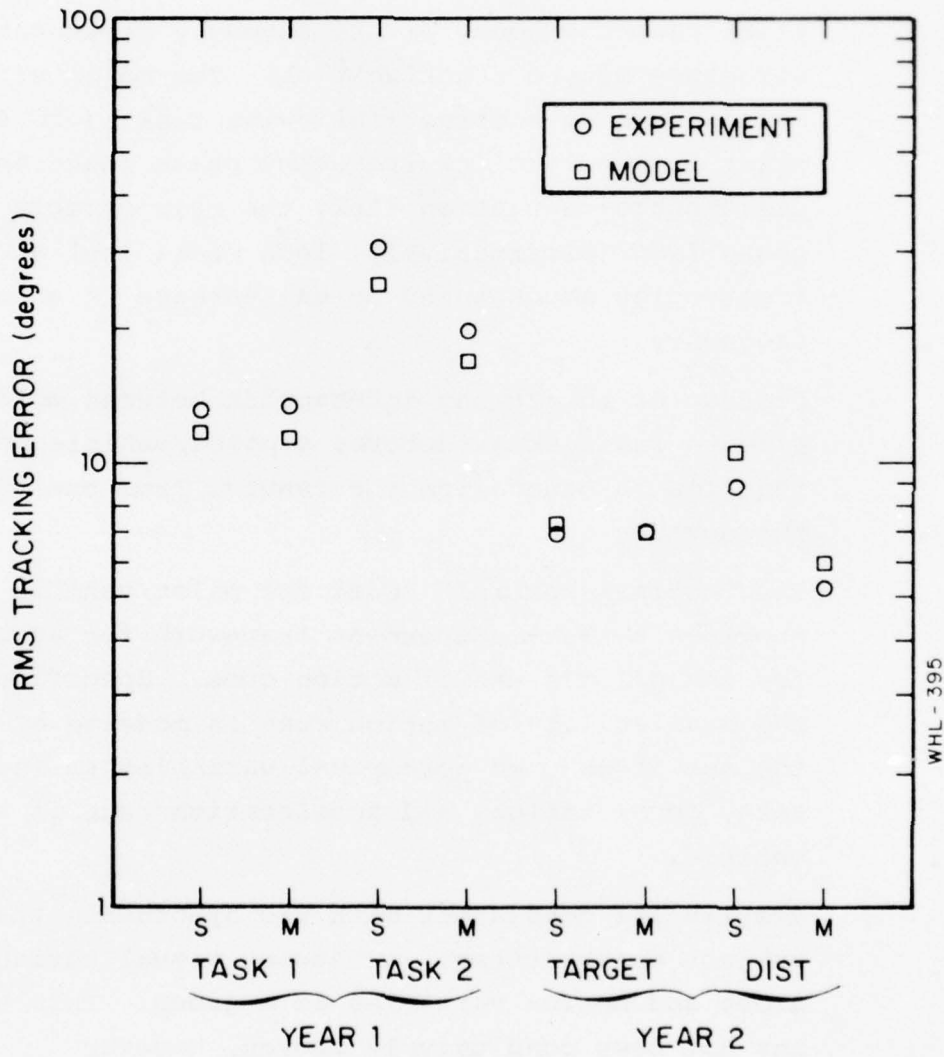


Figure 12. Comparison of Model and Experimental Rms Error Scores for Two Studies  
 S = static condition, M = motion condition.

## 5. CONCLUSIONS

The principal results of this study may be summarized as follows:

1. The effects of motion cues on task performance and pilot response behavior are strongly dependent on the structure of the tracking task. The major effect of motion cues in a target-following task is to allow the pilot to generate low-frequency phase lead; in a disturbance-regulation task, the main effects are more phase lead (alternatively, less phase lag) at high frequencies accompanied by an increase in gain-crossover frequency.
2. Because of the strong interaction between motion-cue effects and task structure, a pilot/vehicle model is required to generalize the results from one task to the next.
3. The "optimal-control" model for pilot/vehicle systems provides a task-independent framework for accounting for the pilot's use of motion cues. Specifically, the availability of motion cues is modeled by augmenting the set of assumed perceptual variables to include position, rate, acceleration, and acceleration rate of the moving vehicle.
4. Results are consistent with the hypothesis that the subject shares attention between visual variables as a group and motion variables as a group. This hypothesis has not been conclusively proven, however.
5. Variations in model parameters relating to motion-cue availability and attention-sharing as described above are sufficient to enable the model to replicate the effects of motion on all performance metrics for the tasks explored in this study.

6. Using the model for motion-cue utilization defined above, plus a single "typical" set of pilot-related model parameters, one can obtain accurate model predictions of rms tracking error scores for all task configurations explored in this study and in the preceding study.
7. There is some evidence that low-quality acceleration information can be obtained directly from the visual display in some tasks. The influence of such information processing on tracking performance appears to be minimal, however.
8. Use of acceleration-rate information appears to allow a modest reduction in rms tracking error in some tasks.
9. Results are consistent with existing models for motion perception by vestibular sensors. Such models are not needed to explain the data obtained in this study, however.

APPENDIX A  
ANALYSIS PROCEDURES

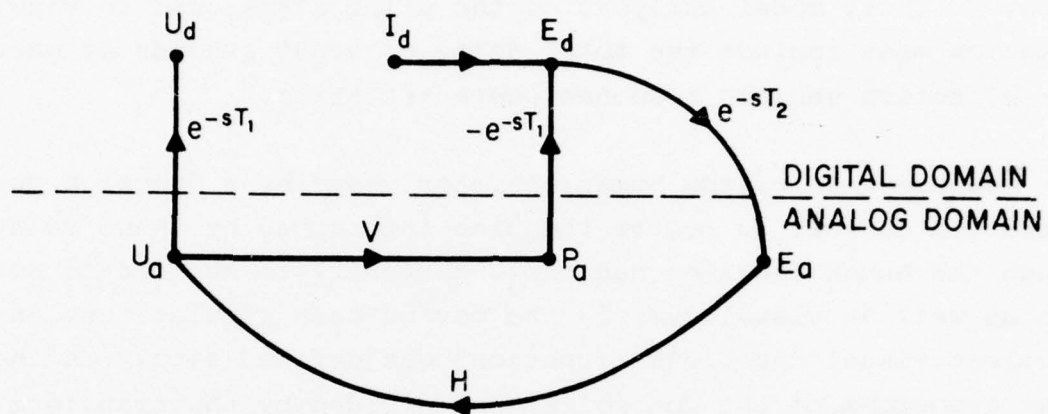
This Appendix describes certain details of the data analysis procedures: specifically (1) treatment of delays introduced in data recording and simulation algorithms, and (2) computation of vehicle acceleration.

A.1 Treatment of Simulation and Computational Delays

Because the simulation involved both analog and digital computation, delays were unavoidably introduced into the tracking loop as well as into the measurement of pilot describing function. Figure A-1 shows the principal sources and locations of delays that were important in the target-following tracking task. (Analysis of the disturbance-regulation task is similar and is not discussed separately.)

The pilot manipulated a control stick, which generated an analog output that was fed directly to the (analog) simulated vehicle. Both the stick and plant outputs were filtered through identical second-order Butterworth filters and digitized. The filter frequency was 40 rad/sec; for purposes of analysis, filter response has been approximated by a pure delay ( $T_1$ ) of 0.040 seconds.

The digitized plant response was differenced with the digitally-generated tracking input to form the tracking error, which was then displayed to the pilot. Simulation delays ( $T_2$ ) on the order of 0.055 seconds were associated with computation and display generation and are shown as such in Figure A-1.



- E = TRACKING ERROR
- H = EQUIVALENT HUMAN OPERATOR RESPONSE TO VISUAL INPUTS
- I = TRACKING INPUT
- P = PLANT POSITION
- s = LAPLACE FREQUENCY VARIABLE
- T<sub>2</sub> = EFFECTIVE DISPLAY AND COMPUTATIONAL DELAY
- T<sub>1</sub> = EFFECTIVE RECORDING DELAY
- U = PILOT'S CONTROL INPUT
- V = VEHICLE DYNAMIC RESPONSE CHARACTERISTICS
- "a" = SIGNIFIES ANALOG DOMAIN
- "d" = SIGNIFIES DIGITAL DOMAIN

WHL-396

Figure A-1. Flow Diagram of the Tracking Task

It is clear from Figure A-1 that both recording and simulation delays appear in the tracking loop insofar as the visual display is concerned. (Note that motion cues are obtained directly from plant motion and are not affected by either source of delay.) Thus, model analysis of the pilot's response to visual information must include the total delay of 0.095 seconds as part of the effective vehicle response characteristics.

Measurements of the human operator describing function must be corrected as well to remove the bias introduced by these delays. Although the human operator had the opportunity to respond to both motion as well as visual cues in the moving-base simulations, an "equivalent visual describing function" was defined simply as the Fourier transform of the control signal divided by the transform of the error signal. The uncorrected describing function ( $H'$ ) was computed as follows:

$$U_d = \frac{-I_d \cdot e^{-sT_2} H e^{-sT_1}}{1 + HV e^{-s(T_1+T_2)}} \quad (A-1)$$

$$E_d = \frac{-I_d}{1 + HV e^{-s(T_1+T_2)}} \quad (A-2)$$

$$H' \equiv \frac{U_d}{E_d} = H \cdot e^{-s(T_1+T_2)} \quad (A-3)$$

Thus, the computed human operator describing function is biased by the same delay that is added to the effective vehicle dynamics. Therefore, all experimental phase-shift data presented in this report have been corrected by a phase lead corresponding to a time advance of 0.095 seconds.

## A.2 Estimation of Plant Acceleration

As direct measurement of vehicle acceleration was not available, estimates of acceleration had to be computed from other measurements. Two procedures were adopted for estimating acceleration: one for obtaining an instantaneous estimate of the total "cost," the other for obtaining a post-experiment estimate.

### A.2.1 Instantaneous Estimate of Acceleration

The plant output was related to control input as

$$\phi = U \cdot 10 \cdot \frac{5}{s+5} \cdot \frac{20}{s+20} \cdot \frac{1}{s} \quad (\text{A-4})$$

where the terms are written to designate the order of signal flow. That is, the pilot's control force was amplified by a factor of 10, filtered by the dynamics of  $5/(s+5)$  to represent high-performance aircraft roll characteristics, filtered again by  $20/(s+20)$  (the approximate dynamics of the moving-base simulator), and finally integrated to convert roll-rate to roll angle. In the static tasks, the final filtering and integration were performed by the analog simulator; in the motion case, these operations were performed directly by the moving-base simulator.

An estimate of plant acceleration was obtained from the portion of the simulation representing aircraft dynamics. The output of this simulation element was computed as

$$x = \frac{50 U - 5 x}{s} \quad (\text{A-5})$$

Since this operation was performed on the analog computer, and not by a moving physical device, the input to the integrator generating the signal "x" was available. This signal,  $\dot{x}$ , was related to the control input as follows:

$$\dot{x} = \frac{50 s}{s+5} U \quad (A-6)$$

and was therefore related to the plant position as

$$\dot{x} = \frac{s+20}{20} s^2 \phi \quad (A-7)$$

Since most of the pilot's response power was concentrated at frequencies below 20 rad/sec, the measurement of  $\dot{x}$  was considered to provide a reliable estimate of vehicle acceleration.

#### A.2.2 Post-Experiment Estimate of Acceleration

For purposes of post-experiment analysis of performance, an estimate of acceleration was obtained by scaling the power spectrum of the plant by  $\omega^4$ , scaling again by the magnitude of the transfer function of a second-order Butterworth filter having a break frequency at 10 rad/sec, and integrating the resulting spectrum. (The filtering was imposed to reduce contributions of high-frequency noise inherent in the differentiation process.) On the average, the two methods of estimating plant acceleration differed by less than 7%.

APPENDIX B  
ADDITIONAL EXPERIMENTAL RESULTS

This Appendix contains additional data to supplement the discussion in Section 4 of the recent roll-axis tracking study. Tables B-1 and B-2 give across-subject means and standard deviations of performance costs and rms performance scores, respectively. Statistics of frequency-response measures are given in Tables B-3 through B-5. "Significance levels" indicate alpha levels of significance for motion-static differences; differences significant at levels greater than 0.05 are considered not significant (NS).

Table B-1  
Effect of Motion Cues on Performance Costs

Variable	Static		Motion		Significance Level
	Mean	Std Dev	Mean	Std Dev	

a. Target Input

Total Cost	73.3	8.30	65.4	4.75	.05
Error Cost	51.0	11.8	47.1	9.38	NS
Acceleration Cost	22.2	8.27	18.3	7.50	NS

b. Disturbance Input

Total Cost	196	26.3	78.6	14.3	.001
Error Cost	81.3	31.3	20.5	14.2	.01
Acceleration Cost	115	34.1	58.1	6.24	.01

Table B-2  
Effect of Motion Cues on Rms Performance Scores

Variable	Static		Motion		Significance Level
	Mean	Std Dev	Mean	Std Dev	

a. Target Input

Error	7.08	.781	6.84	.674	NS
Error Rate	11.9	.768	11.8	.792	NS
Control	.758	.108	.669	.152	.05
Control Rate	2.22	.566	1.99	.482	NS
Plant	9.25	.953	7.50	1.20	.001
Plant Rate	7.12	1.05	6.74	1.71	NS
Plant Acceleration	14.1	2.20	15.3	3.37	NS

b. Disturbance Input

Error	8.82	1.68	4.24	1.44	.01
Error Rate	11.9	1.31	6.81	1.44	.01
Control	1.55	.119	1.49	.067	NS
Control Rate	3.79	1.27	3.82	.689	NS
Plant Acceleration	31.9	3.41	23.5	1.72	.01

Table B-3  
Effect of Motion Cues on Pilot Describing Function,  
Target Input

Frequency (rad/sec)	Static		Motion		Significance Level
	Mean	Std Dev	Mean	Std Dev	

a. Amplitude Ratio (dB)

0.19	-21.3	2.4	-26.7	3.4	.001
0.5	-21.2	2.0	-21.6	3.2	NS
1.0	-20.4	1.5	-21.2	2.8	NS
1.4	-19.9	1.3	-20.8	2.6	NS
2.0	-19.2	1.6	-20.3	2.3	NS
2.8	-18.5	1.7	-20.1	2.2	.05
4.0	-16.8	2.0	-19.1	2.9	.05
5.7	-14.7	3.2	-17.3	3.4	.01
8.0	-12.5	4.7	-16.0	4.1	.05
11	-13.1	5.7	-16.5	3.9	.05
16	-16.3	5.8	-18.9	4.0	NS
22	-21.5	6.0	-21.6	3.6	NS

b. Phase Shift (Degrees)

0.19	-2	10	72	23	.001
0.5	1	10	28	9	.001
1.0	-1	12	8	10	.05
1.4	-2	13	1	13	NS
2.0	-7	15	-8	15	NS
2.8	-14	18	-19	17	.05
4.0	-25	18	-34	18	.05
5.7	-51	24	-59	17	NS
8.0	-95	23	-105	17	.05
11	-159	15	-166	16	.01
16	-244	15	-249	12	NS
22	-335	16	-352	12	.05

0 dB represents 1 pound control force per degree roll error

Table B-4  
Effect of Motion Cues on Pilot Describing Function,  
Disturbance Input

Frequency (rad/sec)	Static		Motion		Significance Level
	Mean	Std Dev	Mean	Std Dev	

a. Amplitude Ratio (dB)

0.19	-15.4	1.5	-7.6	4.2	.05
0.5	-15.9	1.8	-8.3	3.5	.05
1.0	-15.5	2.1	-8.3	3.1	.01
1.4	-15.1	2.1	-7.8	3.1	.01
2.0	-14.6	2.3	-7.9	3.6	.05
2.8	-13.6	2.3	-8.0	3.6	.05
4.0	-11.3	2.1	-7.0	3.3	.05
5.7	-7.3	2.8	-5.3	3.0	NS
8.0	-0.1	4.5	-2.3	2.6	NS
11	-	-	2.0	2.4	NS

b. Phase Shift (Degrees)

0.19	-5	5	-4	10	NS
0.5	-3	9	1	13	NS
1.0	-2	10	7	13	.05
1.4	-1	10	10	12	.05
2.0	-2	11	15	10	.01
2.8	-6	11	21	7	.001
4.0	-11	13	34	7	.001
5.7	-34	23	45	4	.001
8.0	-85	33	52	3	.001
11	-	-	49	5	.001

0 dB represents 1 pound control force per degree roll error

Table B-5  
Effect of Motion Cues on Remnant Ratio

Frequency (rad/sec)	Static		Motion	
	Mean	Std Dev	Mean	Std Dev

a. Target Input

0.19	-17.9	1.5	-12.0	2.5
0.5	-17.1	2.9	-15.2	2.0
1.0	-12.7	1.3	-12.0	2.3
1.4	-11.2	0.7	-9.3	2.0
2.0	-8.4	1.9	-6.0	2.0
2.8	-5.3	1.7	-2.8	2.3
4.0	-3.6	1.4	0.2	2.8
5.7	-1.0	2.1	2.8	3.9
8.0	0.4	2.0	4.1	3.0
11	3.6	2.4	6.8	3.1
16	6.6	2.6	9.3	2.4
22	12.5	2.3	13.8	1.2

b. Disturbance Input

0.19	-29.5	3.1	-31.5	2.5
0.5	-21.7	2.2	-26.4	3.5
1.0	-15.1	2.0	-19.0	3.2
1.4	-11.8	2.3	-16.4	3.2
2.0	-8.6	2.1	-12.5	2.9
2.8	-4.6	1.5	-8.2	3.3
4.0	-0.5	1.5	-3.8	2.8
5.7	4.4	1.3	0.5	2.8
8.0	8.3	0.5	3.5	2.3
11	-	-	7.3	1.8

Remnant ratios in dB (dimensionless ratio)

## APPENDIX C

### MODEL FORMULATION

Certain details related to applying the optimal-control pilot/vehicle model are described in this Appendix. Results of the model analysis are discussed in Section 4.2

#### C.1 System Dynamics

Equations of motion describing vehicle, input and sensor dynamical response characteristics are described below.

##### C.1.1 Target-Following Task

The system dynamics relating plant output (roll angle) to control input were:

$$\frac{P(s)}{U(s)} = \frac{10}{s} \cdot \frac{5}{s+5} \cdot \frac{20}{s+20} \quad (c-1)$$

The (analytic) input signal assumed for this task was

$$\phi_{ii}(s) = \left| \frac{2.0}{(s+1)^2} \right|^2 W \quad (C-2)$$

where  $W$  is a white noise process having a variance equal to the variance of the tracking input ( $100 \text{ deg}^2$  in this experiment). The input was assumed to be differenced from the plant output to produce the tracking error, and this error was assumed displayed to the pilot after a delay of 0.095 seconds to account for recording and simulation lags. The delay was approximated by the following first-order Pade network:

$$E = \frac{-s + 21.1}{s + 21.1} E' \quad (C-3)$$

where  $E'$  is the underlayed error,  $E$  is the error as displayed to the pilot.

The following equations for state and output variables were used in the model analysis:

$$\begin{aligned} \dot{x}_1 &= -2.0 x_1 - 1.0 x_2 + 2.0 w \\ \dot{x}_2 &= 1.0 x_1 \\ \dot{x}_3 &= -5.0 x_3 + 50 u \\ \dot{x}_4 &= 20 x_3 - 20 x_4 \\ \dot{x}_5 &= 1.0 x_4 \\ \dot{x}_6 &= 1.0 x_1 - 21.2 x_2 - 1.0 x_4 + 21.1 x_5 - 21.1 x_6 \\ y_1 &= 1.0 x_6 \\ y_2 &= 1.0 x_1 - 21.1 x_2 - 1.0 x_4 + 21.1 x_5 - 21.1 x_6 \\ y_3 &= 1.0 x_5 \\ y_4 &= 1.0 x_4 \\ y_5 &= 20 x_3 - 20 x_4 \\ y_6 &= -5.0 x_3 + 50 u \\ y_7 &= -500 x_3 + 400 x_4 + 1000 u \end{aligned}$$

where:

$$\begin{aligned} x_1 &= \text{input rate} \\ x_2 &= \text{input} \\ x_3 &= \text{internal state} \\ x_4 &= \text{plant rate} \\ x_5 &= \text{plant position} \\ x_6 &= \text{tracking error} \end{aligned}$$

y1 = tracking error  
 y2 = tracking error rate  
 y3 = plant position  
 y4 = plant rate  
 y5 = plant acceleration  
 y6 = approximation to plant acceleration  
 y7 = plant acceleration rate

The approximate acceleration variable y6 was defined in order to provide a model variable to correspond to the approximate measure of acceleration used experimentally to compute performance cost. (See Appendix A.) The cost functional used in obtaining model solutions was

$$J = 1.0 \sigma_{y1}^2 + 0.05 \sigma_{y6}^2 + 1.00 \sigma^2 \dot{u} \quad (C-4)$$

The coefficient 0.05 operating on y6 was selected to match the experimental data, and the coefficient 1.00 operating on control-rate variance was the value that yielded a "motor time constant" of 0.1 seconds.

#### C.1.2 Disturbance-Regulation Task

The relationship between plant output and control input was identical to that shown in Equation (C-1). The tracking input assumed for this task was

$$\phi_{ii}(s) = \left| \frac{5.657}{(s+2)^2} \right|^2 W \quad (C-5)$$

where, for this task, W represents a white noise process having a variance of  $196 \text{ (deg/sec)}^2$ .

The tracking input was added to the pilot's control input (the latter having been scaled by a factor of 10); the computational delay associated with visual presentation of tracking error was approximated by the Pade network of Equation (C-3).

The following state and output equations resulted:

$$\begin{aligned}\dot{x}_1 &= -4.0 x_1 - 4.0 x_2 + 5.657 w \\ \dot{x}_2 &= 1.0 x_1 \\ \dot{x}_3 &= 5.0 x_2 - 5.0 x_3 + 50 u \\ \dot{x}_4 &= 20 x_3 - 20 x_4 \\ \dot{x}_5 &= 1.0 x_4 \\ \dot{x}_6 &= -1.0 x_4 + 21.1 x_5 - 21.1 x_6\end{aligned}$$

$$\begin{aligned}y_1 &= 1.0 x_6 \\ y_2 &= -1.0 x_4 + 21.1 x_5 - 21.1 x_6 \\ y_3 &= -20 x_3 + 62.2 x_4 - 445 x_5 + 445 x_6 \\ y_4 &= 1.0 x_5 \\ y_5 &= 1.0 x_4 \\ y_6 &= 20 x_3 - 20 x_4 \\ y_7 &= 5.0 x_2 - 5.0 x_3 + 50 u \\ y_8 &= 100 x_2 - 500 x_3 + 400 x_4 + 1000 u\end{aligned}$$

where the state variables are as defined above for the target-following task, and the display variables are

$$\begin{aligned}y_1 &= \text{tracking error} \\ y_2 &= \text{tracking error rate} \\ y_3 &= \text{tracking error acceleration} \\ y_4 &= \text{plant position} \\ y_5 &= \text{plant rate}\end{aligned}$$

$y_6$  = plant acceleration  
 $y_7$  = approximation to plant acceleration  
 $y_8$  = plant acceleration rate.

The following models were adopted for the semicircular canals and otolith motion sensors:

$$Y_s = \frac{188(.02s + 1)}{(18s + 1)(30s + 1)} \ddot{\phi} \quad (C-5)$$

$$Y_o = \frac{91.1(s + .0988)}{(s + 0.2)} SF \quad (C-6)$$

where SF is the specific force. As discussed in Section 4.2.4, SF may be approximated for these experiments as

$$SF = \phi - 0.093 \ddot{\phi} \quad (C-7)$$

The subject was assumed to perceive the sensor outputs  $y_s$  and  $y_o$ , as well as the derivatives of these variables. These vestibular dynamics were incorporated in the overall system model by expanding the state and display equations as follows:

$$\begin{aligned}
 \dot{x}_7 &= 1.0 x_8 \\
 \dot{x}_8 &= 20 x_3 - 20 x_4 - 0.00185 x_7 - 0.089 x_8 \\
 \dot{x}_9 &= -0.372 x_3 + 0.372 x_4 + 0.20 x_5 - 0.2 x_9 \\
 y_9 &= 0.139 x_3 - 0.139 x_4 - .129 \times 10^{-5} x_7 + 3.74 x_8 \\
 y_{10} &= 0.696 x_2 + 4.0 x_3 - 4.70 x_4 - 6.92 \times 10^{-4} x_7 \\
 &\quad - 0.0333 x_8 + 6.96 u \\
 y_{11} &= -169 x_3 + 169 x_4 + 91.4 x_5 - 46.1 x_9 \\
 y_{12} &= -846 x_2 + 4247 x_3 - 3310 x_4 - 9.22 x_5 + 9.22 x_9 - 8460 u
 \end{aligned}$$

where  $x_7 - x_9$  are states related to motion sensor dynamics,  
and

$y_9$  = output of semicircular canal sensor

$y_{10}$  = rate of change of output of semicircular canal sensor

$y_{11}$  = output of otolith sensor

$y_{12}$  = rate of change of output of otolith sensor

## C.2 Display Analysis

Resolution limitations of perception are accounted for in the pilot/vehicle model through appropriate adjustment of observation noise levels. An effective perceptual "threshold" is determined for each displayed variable; the smaller the predicted rms level of a given quantity, the greater the variance of the associated observation noise process. Additional details on treatment of perceptual thresholds may be found in [13].

Effective thresholds for the model analysis performed in this study were computed on the basis of the following assumptions:

1. Thresholds are determined by the subject's ability to perceive displacement and rate of the tip of the rotating error bar.
2. On the basis of previous studies [11], effective perceptual thresholds for displacement and rate are approximately 0.05 degrees visual arc and 0.2 degrees/second visual arc, respectively.

In order to relate degrees visual arc as seen by the pilot to degrees of rotation of the error bar, the following measurements are needed:

$$L = 0.625 \text{ inches}$$

$$D = 20 \text{ inches}$$

where L is the length of the error bar from center to tip and D is the distance from the subject's eye to the display.

We define the following variables:

S = displacement of the tip of the error bar in inches

$\phi$  = angle of displacement of the error bar, degrees

$\alpha$  = displacement of the tip of the error bar in degrees visual arc

and note the following relationships:

$$\tan \alpha = S/D \tag{C-8}$$

$$\tan \phi = S/L$$

If we assume angles small enough so that the tangent of the angle is approximately equal to the angle (in radians), the following relationship applies:

$$\phi = \frac{D}{L} \alpha = 32 \alpha \tag{C-9}$$

Thus, in terms of problem units, effective perceptual thresholds are 1.6 degrees and 6.4 degrees/second.

Model analysis was initially performed using these values for perceptual thresholds. A closer match to experimental data was obtained, however, by ignoring the displacement threshold and reducing the rate threshold by half.

It should be noted that the values initially assumed for perceptual thresholds are based on studies in which the subjects' visual task was to estimate the *translation* of the error bar from a zero-reference bar. Different perceptual processes may have been involved in this study, as the subjects were required to detect *rotation* of the error bar. Additional laboratory studies would seem to be in order to determine more precisely the effective thresholds that correspond to perception of rotational displacement and velocity in manual control tasks.

#### REFERENCES

1. Levison, W. H., S. Baron, and A. M. Junker, "Modeling the Effects of Environmental Factors on Human Control and Information Processing," AMRL-TR-76-74, Aerospace Medical Research Laboratory, Wright-Patterson AFB, Ohio, Aug 76. [AD A-030585]
2. Levison, W. H., "Use of Motion Cues in Steady-State Tracking," Twelfth Annual Conference on Manual Control, NASA Technical Memorandum, NASA TM X-73,170, pp. 895-917, May 1976.
3. Peters, R. A., "Dynamics of the Vestibular System and Their Relation to Motion Perception, Spatial Disorientation, and Illusions," NASA CR-1309, April 1969.
4. Young, L. R., "The Current Status of Vestibular System Models," Automatica, Vol. 5, pp. 369-383, 1969.
5. Levison, W. H. and P. D. Houck, "Guide for the Design of Control Sticks in Vibration Environments," AMRL-TR-74-127, Aerospace Medical Research Laboratory, Wright-Patterson AFB, Ohio, February 1975. [AD A-008533]
6. Levison, W. H., "Biomechanical Response and Manual Tracking Performance in Sinusoidal, Sum-of-Sines, and Random Vibration Environments," AMRL-TR-75-94, Aerospace Medical Research Laboratory, Wright-Patterson AFB, Ohio, April 1976. [AD A-026286]
7. Shirley, R. S., "Motion Cues in Man-Vehicle Control," M.I.T., Cambridge, Massachusetts, Sc.D. Thesis, January 1968.
8. Stapleford, R. L., R. A. Peters and F. Alex, "Experiments and a Model for Pilot Dynamics with Visual and Motion Inputs," NASA CR-1325, May 1969.
9. Junker, A. M. and W. H. Levison, "Recent Advances in Modelling the Effects of Roll Motion on the Human Operator," presented at Symposium on Biodynamic Models and their Applications, Bergamo Center, Dayton, Ohio, February 15-17, 1977.
10. Junker, A. M. and W. H. Levison, "Use of the Optimal-Control Pilot Model in the Design of Experiments," to be published in the Proceedings of the Thirteenth Annual Conference on Manual Control, MIT, Cambridge, Mass., June 15-17, 1977.
11. Levison, W. H., "The Effects of Display Gain and Signal Bandwidth on Human Controller Remnant," AMRL-TR-70-93, Wright-Patterson AFB, Ohio, March 1971. [AD 727057]

REFERENCES (Cont'd.)

12. R. E. Curry, W. C. Hoffman, and L. R. Young, "Pilot Modeling for Manned Simulation," AFFDL-TR-76-124, Volume I, Final Report April 1975 - June 1976, Air Force Flight Dynamics Laboratory, Wright-Patterson AFB, Ohio, December 1976.
13. S. Baron and W. H. Levison, "An Optimal Control Methodology for Analyzing the Effects of Display Parameters on Performance and Workload in Manual Flight Control," IEEE Trans. on Systems, Man, and Cybernetics, Vol. SMC-5, No. 4, July 1975.